National Library of Canada
Bibliothèque nationale du Canada

Canadian Theses Service
Service des thèses canadiennes

Ottawa, Canada
K1A 0N4

NOTICE

The quality of this microform is heavily dependent upon the quality of the original thesis submitted for microfilming. Every effort has been made to ensure the highest quality of reproduction possible.

If pages are missing, contact the university which granted the degree.

Some pages may have indistinct print especially if the original pages were typed with a poor typewriter ribbon or if the university sent us an inferior photocopy.

Reproduction in full or in part of this microform is governed by the Canadian Copyright Act, R.S.C. 1970, c. C-30, and subsequent amendments.

AVIS

La qualité de cette microforme dépend grandement de la qualité de la thèse soumise au microfilmage. Nous avons tout fait pour assurer une qualité supérieure de reproduction.

S'il manque des pages, veuillez communiquer avec l'université qui a conféré le grade.

La qualité d'impression de certaines pages peut laisser à désirer, surtout si les pages originales ont été dactylographiées à l'aide d'un ruban usé ou si l'université nous a fait parvenir une photocopie de qualité inférieure.

La reproduction, même partielle, de cette microforme est soumise à la Loi canadienne sur le droit d'auteur, SRC 1970, c. C-30, et ses amendements subséquents.

NL-339 (r. 88/04) c

Canada

Permission has been granted to the National Library of Canada to microfilm this thesis and to lend or sell copies of the film.

The author (copyright owner) has reserved other publication rights, and neither the thesis nor extensive extracts from it may be printed or otherwise reproduced without his/her written permission.

L'autorisation a été accordée à la Bibliothèque nationale du Canada de microfilmer cette thèse et de prêter ou de vendre des exemplaires du film.

L'auteur (titulaire du droit d'auteur) se réserve les autres droits de publication; ni la thèse ni de longs extraits de celle-ci ne doivent être imprimés ou autrement reproduits sans son autorisation écrite.

ISBN 0-315-56461-X

USE OF LIQUID CHROMATOGRAPHY IN MEMBRANE MATERIAL CHARACTERIZATION

A Thesis
submitted to the Department of Chemical Engineering
and the School of Graduate Studies
of the University of Ottawa
in Partial Fulfillment of the Requirements
for the Degree of
Master of Applied Science

by
Chung Ming Tam
January 1989

© Chung Ming Tam, Ottawa, Canada, 1989

UNIVERSITÉ D'OTTAWA
UNIVERSITY OF OTTAWA

© Copyright 1989

by

Chung Ming Tam

Abstract

Membrane separations are a manifestation of the surface forces at the membrane-solution interface. The surface interactions in a liquid chromatography system are analogous to those present in a membrane-solution system. The retention time of a solute passing through a chromatography column is a direct measure of the attraction or repulsion between a solute and the polymer in an aqueous environment. These interactions are described as a function of solute properties such as hydrophilicity and molecular size. The interactions are also a function of the polymer properties and these properties can be quantified by Hansen's solubility parameters. The results from liquid chromatography experiments are used to explain why functional polymers can produce membranes with higher performance than commercially available polymers.

Acknowledgements

The author wishes to express his appreciation and gratitude to Professors F. D. F. Talbot, T. Matsuura, and Mr. O. Kutowy for their suggestions and guidance throughout this research project. The author also wishes to thank Mr. A. Y. Tremblay for his help and advice.

The financial support of Zenon Environmental Inc. under a contract (Number 31949-6-0003/01-SZ) from the Biotechnology Research Institue of the National Research Council is gratefully acknowledged. The equipment and the technical support provided by the Chemical Engineering section of the National Research Council are also deeply appreciated.

Finally, the author wishes to thank his parents and sisters for their patience and encouragement during the course of this project.

Contents

List of Tables

List of Figures

Chapter 1

Introduction

1.1 Membrane Separation Processes

Membrane separation is based on the principle that components of gaseous or liquid mixtures will pass through or permeate a microporous surface at different rates due to molecular interactions between the membrane, the solute, and the solvent.

Molecular interactions by definition can encompass a variety of different phenomena. The term interaction can include interfacial forces exerted on the components of the mixture by the surface, the kinetic effect of friction as molecules move through pores within the solid as well as physical effects such as size exclusion of the solute from the membrane pores. The importance of each of these effects depends on the particular membrane-solute-solvent system.

Membrane separation processes for liquid systems are traditionally sub-divided into different categories according to the size of the solute in the solution. Figure 1 illustrates such a classification scheme [1]. The definitions are not rigorous or universal and there is a tendency for each section to overlap.

Molecular sieving action plays a pivotal role in a separation when there is a large difference in molecular size between components in the solution; such conditions exist in the realm of microfiltration and ultrafiltration. Surface interactions become progressively more important and eventually dominate as both the solute size and the pore diameter decrease. The nature of the membrane interface influences the

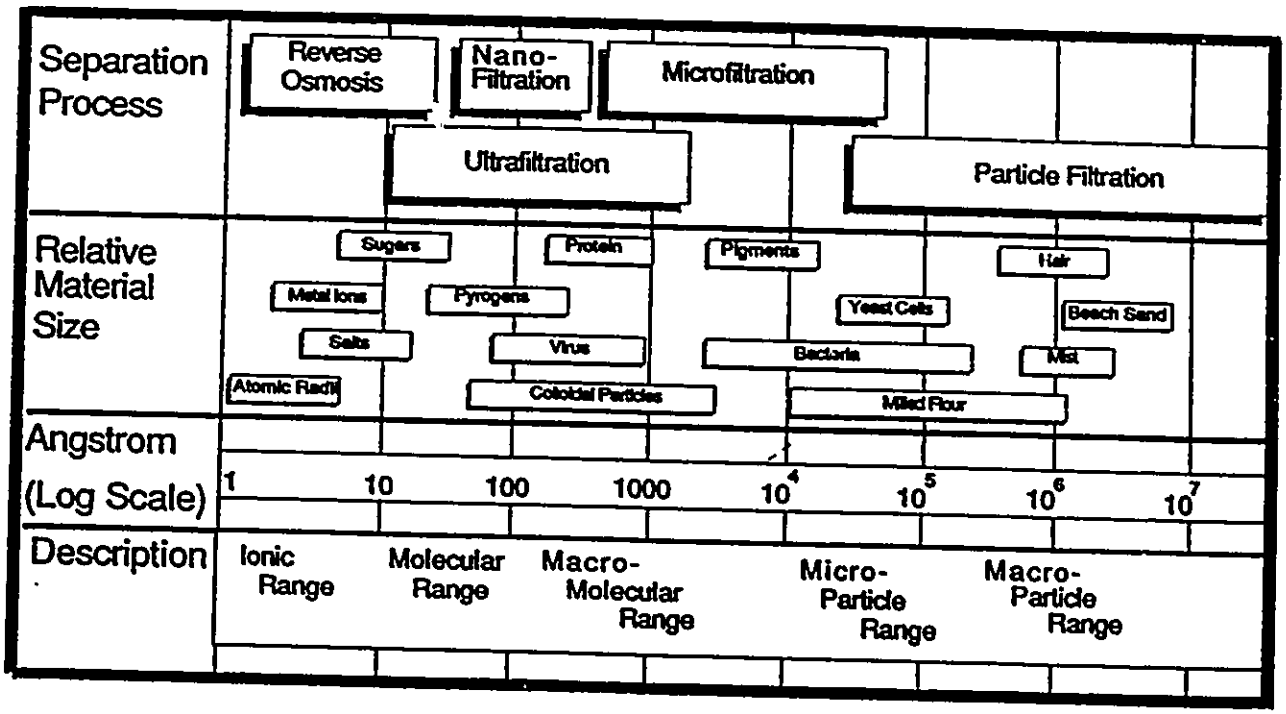

Figure 1: The range of membrane based separation processes

product rate and the solute separation when the process is within the range of nanofiltration, reverse osmosis or membrane based gas separation.

The role of the interfacial forces at the membrane-solution interface can be described by the Gibbs adsorption equation. This equation arose out of thermodynamic considerations and describes the actions at the boundary between any two phases (eg. liquid-gas, liquid-solid, liquid-liquid). Gibbs [2] proposed that a change in surface tension corresponds to a variation in the activity of a system :

$$\Gamma = \frac{-1}{RT}\left(\frac{\partial \gamma}{\partial \ln a}\right)_{T,P} \tag{1}$$

The surface tension (γ) or surface free energy is the additional free energy per unit area caused by the presence of the interface. The surface excess (Γ) can be viewed as a difference in solute concentration between the bulk solution and at the interfacial layer. The activity (a) can be approximated by the concentration (c) for very dilute solutions. The physical interpretation of the Gibbs adsorption equation is the existence of surface forces acting at the boundary of any two phases which produce a concentration gradient between different components in the solution.

Sourirajan established the Preferential Sorption Capillary Flow (PSCF) mechanism for membrane separation based on the vision provided by the Gibbs adsorption equation. The mechanism tries to explain the phenomena of membrane separation as a direct result of a concentration gradient that develops between different components in the solution at the membrane interface. This concentration gradients exists in the form of a interfacial layer of finite thickness. The application of a driving force produces a flow of the interfacial layer through appropriate size pores in the membrane. This results in a permeate composition that is different from the bulk composition. Sourirajan and Loeb were able to produce a commercially viable cellulose acetate desalination membrane in 1960 [3] based on the principle established in the PSCF mechanism. The cellulose acetate membrane material provides the appropriate interface while the pores provide a means of removing the interfacial layer. This idea is best illustrated by figure 2. Water is preferentially attracted at the interface, while sodium chloride is rejected. This results in the formation of a water layer adjacent to the membrane surface. The interfacial layer can then be

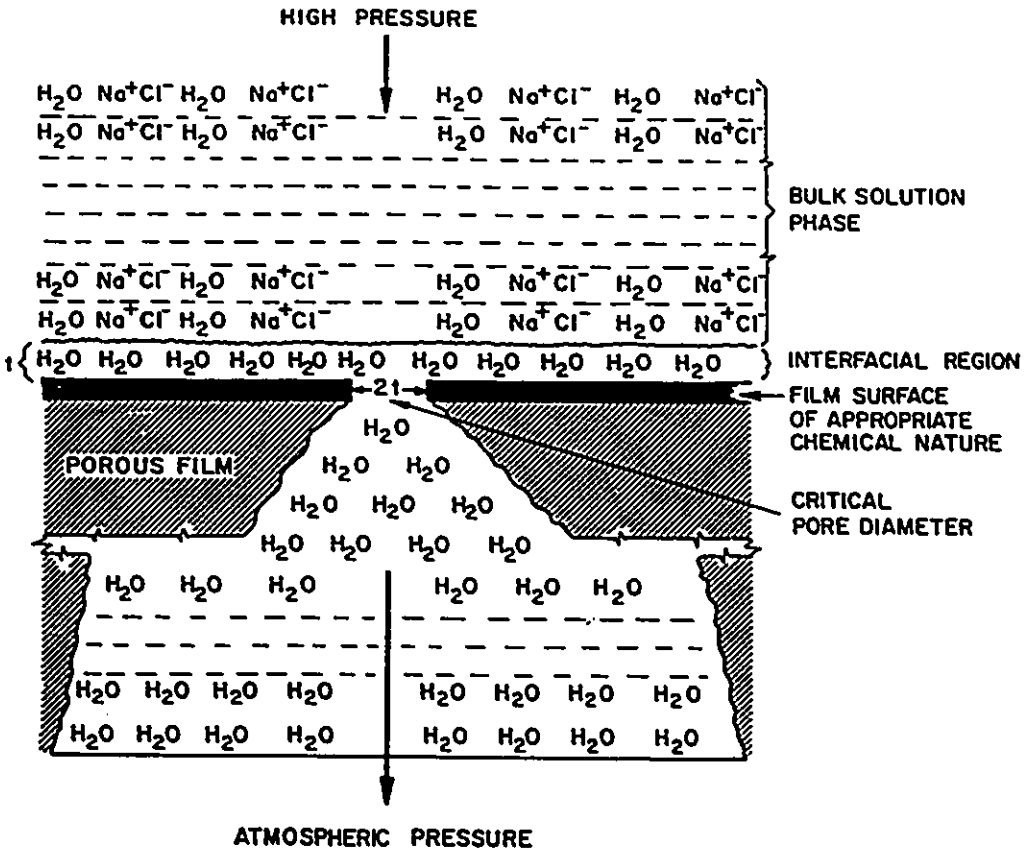

Figure 2: The Surface Force Capillary Flow mechanism applied to Cellulose Acetate-Sodium Chloride-Water system.

removed through an appropriate pore size with the application of pressure. The ideal membrane will then be the one that has a pore radius equal to the thickness of the interfacial water (T_i). The theoretical radius is known as the critical pore radius (r_c). This fundamental concept can be extended to any solution and interface and serves as one of the key factors in understanding the nature of membrane based separations.

The use of membrane processes offers an excellent alternative to conventional separation methods because of the driving force and good selectivity. The driving force for the separation is a pressure gradient. Usually, the feed side (concentrate) has a high pressure while the outlet (permeate) is at atmospheric pressure. The energy involved in membrane separations is usually less intensive than competing operations such as distillation because phase changes are not involved. Membrane processes are now used in areas of concentration, separation and fractionation of heat sensitive materials usually found in the field of biotechnology and food processing. Membrane technology has now become a standard unit operation in chemical engineering.

1.1.1 Membrane Materials

The method of selecting the appropriate interface is only the first step in the design and control of any membrane development. The type of materials that can be made into membranes include available polymers, copolymers, special functional polymers, as well as a variety of inorganic materials such as ceramics. There are no definite criteria for selecting the correct membrane material for the desired separation before actually making and testing the membrane. Currently, trial and error methods and experience are the usual guidelines in selecting the material. There is a need to develop a reliable screening procedure for selecting appropriate membrane materials for a particular separation. The selection should be influenced by the underlying principle of membrane separation. This means that the procedure must reflect the physicochemical interactions of the membrane-solute-solvent system. Liquid chromatography (LC) methods is proposed as the analytical method for classifying and selecting suitable membrane materials. The parallels between

LC systems and membrane-solution systems are later described.

The membrane materials chosen for this study are a family of aromatic polysulfones which are now used commercially in the form of microfiltration and ultrafiltration membranes and as supports for thin film composites and gas separation membranes [4]. There are three types of polysulfones available : Udel (Bisphenol-A-polysulfone), Radel (polyphenylsulfone), and Victrex (polyethersulfone). The chemical structure for each polymer is given in figure 3.

Polysulfones constitute a class of amorphous thermo-plastics that have excellent chemical and physical properties which are ideally suited for membrane production [5]. Polysulfones are inherently strong, tough, and possess good creep resistance. Their chemical structure also gives the polymers protection against extremes in pH as well as high thermal stability. They can withstand temperatures of up to 150°C [6]. This group of polymers has low solubility in aliphatic media but can be attacked by polar solvents such as N-N-Dimethylacetamide (DMA), and chlorinated solvents such as chloroform as well as aromatics such as benzene.

A method developed by Guiver *et al.* [7,8,9,10] can further enhance the applicability of this family of polysulfones by changing the physicochemical nature of the polymer which in turn changes the interaction at the polymer-solute interface. This method consists of the addition of lithium to an active site on the Udel polymer followed by a electrophilic substitution. Polysulfone can be modified regiospecifically at the ortho-sulfone site by this process of lithiation. The choice of electrophile leads to products with different functional groups. These functional groups can be attached directly onto the main chain or attached with spacer to the main chain. Such additions produce new functionalized polymers with active sites attached to their backbone while maintaining the physical and chemical resilience of the unmodified polymer. These pendant side chains can be charged groups (as in the case of ionomers), aliphatic groups or metallic groups [11]. This new class of polymer is a key to enhancing future polysulfone membrane performance. An appropriate substituent group can be introduced onto the polymer material so that surface interactions can be modified to achieve the desired separations.

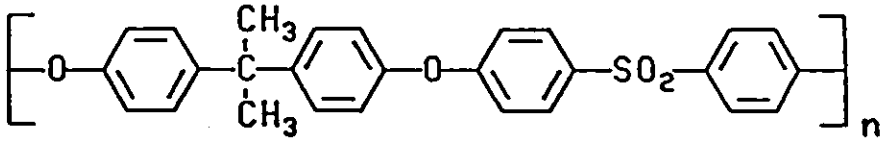

Udel

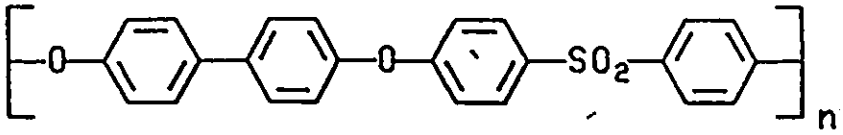

Radel

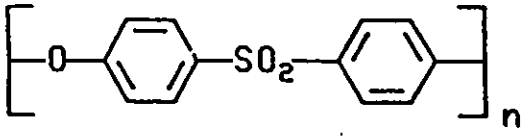

Victrex

Figure 3: Chemical Structure for a Family of Polysulfones

There is a wide choice of substituent groups that can be added onto the polysulfone backbone. The difficulty lies in choosing the appropriate functional group for specific applications. A method must be selected to obtain the maximum amount of information from each derivative since the cost of modifying the polymer is high. LC is proposed as a method to quantitatively analyze the change in polymer surface property, and obtain parameters that can characterize the substituent groups in the system. The two substituent groups that have been chosen for the present work are the carboxylated functional group (CPS) and the trimethylsilyl functional group (TMS). The chemical structures for the two modified Udel polysulfones are given in figure 4.

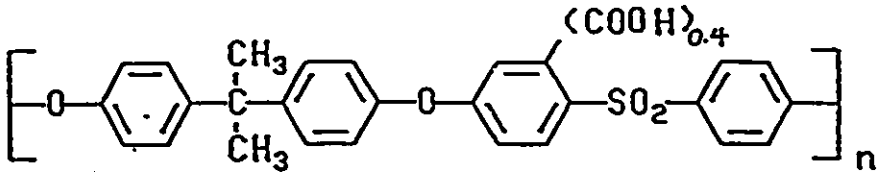

Carboxylated Udel Polysulfones (CPS)

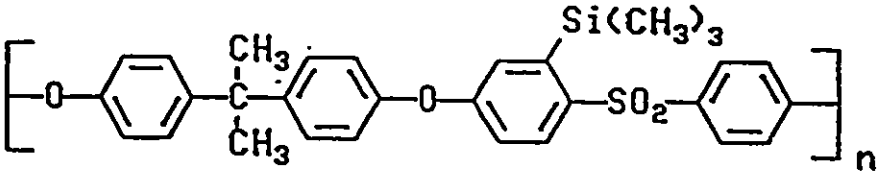

Tri-methylsilyl Udel Polysulfone (TMS)

Figure 4: Chemical Structure for Modified Udel Polysulfones

Chapter 2

Characterization of Membrane Materials

2.1 Surface Force Pore Flow (SFPF) Model

The essential nature of membrane separation has been described in the introduction. Several mathematical models to explain the phenomenon of solute transport have been proposed and are reviewed in the literature [12]. The Surface Force Pore Flow (SFPF) model developed at the National Research Council of Canada [13] takes explicitly into account the effect of surface forces at the solution-membrane interface. The transport of solvent and solute through the surface of a membrane can be described by solute-solvent-membrane interactions acting in conjunction with the physical effect of fluid flow within the membrane pores. This model allows for the prediction of membrane flux and component separation even when the solute is preferentially sorbed.

A brief description of the SFPF model will be useful in demonstrating the importance of surface interaction parameters in solute separation and transport.

The starting point according to the SFPF model is that the separation and permeation are controlled by a porous thin skin layer on the surface of the membrane. The model then assumes the pores on the membrane surfaces can be expressed as equivalent cylindrical capillaries with an associated pore-size distribution. The

solute flux and the velocity profile can be calculated using standard force and momentum balances within the pore.

Based on a force balance, the molar solute flux (J_a) at a distance (r) from the inside wall of the cylindrical pore can be described as [13] :

$$J_a(r) = \frac{-RT}{\chi_{AB}\, b(r)} \left(\frac{\delta c_a(r,z)}{\delta z}\bigg|_{r=r} \right) + \frac{c_a(r,z)\, u_b(r)}{b(r)} \tag{2}$$

where

$c_a(r,z)$ – Solute concentration in the r and z direction
χ_{AB} – Proportionality constant
$b(r)$ – Dimensionless overall friction coefficient
$u_b(r)$ – Velocity of solvent in the pore

Boundary conditions must be defined in order to solve equation 2. The boundaries are the local concentration at the inlet of the pore (c_a(r,0)) and the local concentration at the end of the pore (c_a(r,δ)). These values are obtained by assuming that the Maxwell-Boltzmann distribution law is valid. The local concentration is related to a bulk value (c_{a2}, c_{a3} for the interface layer and the permeate side respectively) by a potential function (ϕ), so that :

$$c_a(r,0) = c_{a2} e^{-\phi(r)/RT} \tag{3}$$

$$c_a(r,\delta) = c_{a3} e^{-\phi(r)/RT} \tag{4}$$

Solution and rearrangement of equation 2 with the corresponding boundary conditions leads to expression 5 for the separation (f') of a membrane in terms of the solute velocity profiles and various interactions parameters :

$$f' = 1 - \left[\left\{ \int_0^R \left(\frac{\exp(\frac{u_b(r)\,\delta\,\chi_{AB}}{RT})}{1 + \frac{b(r)}{e^{-\phi/RT}}} \left\{ \exp(\frac{u_b(r)\,\delta\,\chi_{AB}}{RT}) - 1 \right\} \right) \times (u_b(r)) r dr \right\} \div \left\{ \int_0^R u_b(r) r dr \right\} \right] \tag{5}$$

The radial velocity profile for solvent flow ($u_b(r)$) can be obtained from a momentum balance [13]. A second order differential equation (equation 6) must be solved in order to generate the velocity profile.

$$\frac{d^2u_b(r)}{dr^2} + \frac{1}{r}\frac{du_b(r)}{dr} - \frac{1}{\eta}\frac{\{P(r,\delta) - P(r,0)\}}{\delta} - \frac{\chi_{AM}(r)c_{a3}(r)u_b(r)}{\eta} = 0 \qquad (6)$$

where

P(r,δ)-P(r,0) – Pressure gradient as a function of r

η – Viscous shear forces

χ_{AM} – Solute-membrane interaction constant

Again, in order to solve this equation, a Maxwell-Boltzmann distribution is assumed. The localized pressure at the inlet (P(r,0)) and at the outlet (P(r,δ)) is related to the pressure at the bulk phase (P_i, P_o), a potential function (ϕ) and a bulk concentration (c_{a2}, c_{a3}) :

$$P(r,0) = P_i - RTc_{a2}[1 - e^{-\phi(r)/RT}] \qquad (7)$$

$$P(r,\delta) = P_o - RTc_{a3}[1 - e^{-\phi(r)/RT}] \qquad (8)$$

So that equation 6 can be rewritten as :

$$\begin{aligned} \frac{d^2u_b(r)}{dr^2} &+ \frac{1}{r}\frac{du_b(r)}{dr} + \frac{1}{\eta}\frac{P_i - P_o}{\delta} \\ &+ \frac{1}{\eta}\frac{RT}{\delta}\{c_{a3}(r) - c_{a2}(r)\}[1 - e^{\frac{-\phi(r)}{RT}}] \\ &- \frac{\{b(r) - 1\}\,\chi_{AB}\,c_{a3}(r)\,u_b(r)}{\eta} \qquad (9) \\ &= 0 \qquad (10) \end{aligned}$$

Equations 2 and 10 form the basis for the SFPF model. One of the problems that arise out of the model is the need for a realistic estimate of the potential function. The assumption of a Maxwell-Boltzmann distribution relates bulk values which can be measured to localized values needed in the model :

$$c_{a,i} = c_{a,b}\exp(-\phi(d)/RT) \qquad (11)$$

The form of the potential function ($\phi(d)$) for the Maxwell-Boltzmann relationship is inversely proportional to the distance from the membrane wall for ionized solutes (equation 12).

$$\phi(d) = \begin{cases} \infty & \text{when d < D} \\ \frac{A}{d} & \text{when d > D} \end{cases} \tag{12}$$

where

A – Electrostatic repulsive force constant

d – Distance between the membrane surface and the solute molecule

D – Distance at which ϕ becomes very large due to steric hindrance of the solvent molecule

A Leonard-Jones potential function is assumed for non-ionized solutes (equation 13):

$$\phi(d) = \begin{cases} \infty & \text{when d < D} \\ -\frac{B}{d^3} & \text{when d > D} \end{cases} \tag{13}$$

where

B – Attraction constant for a Leonard-Jones potential function

The development of the transport model leads to a need to quantify surface interactions. An assumption of a Maxwell-Boltzmann distribution requires the ability to generate a potential function that is specific to the solute and to the membrane material. Data other than those obtained from membrane separation experiments must be introduced.

2.2 Methods to obtain Surface Interactions

There are only three values that can be obtained from any one membrane separation experiment. These are :

- Pure solvent permeation rate (PWP)
- Permeation rate of the solution through the membrane (PR)

- Difference in composition (percent separation) between the bulk solution and the permeate solution.

Together, these quantities describe both the physical influence of the pore and pore size as well as the surface effects of the membrane . Data from any one membrane separation experiment cannot distinguish between the contribution of the pore and the contribution of the surface forces to the solute separation and flux. A series of membrane experiments use to decouple the effect of the pore and the effect of the polymer are both complicated and time consuming. A direct means of evaluating the solute-solvent-membrane interactions must be found.

Dense film permeation is one method often used to reveal the effect of the polymer surface [14]. A dense film is produced by complete solvent evaporation of a membrane casting solution at high temperature or for long evaporation time. This dense film will not have the skin layer normally associated with an asymmetric membrane. It is then placed between a concentrated solution and a pure solvent stream. The change in concentration due to osmosis is recorded. This experiment provides the permeation rate of the solute under a concentration gradient. The disadvantage of this process is that a transport model must be assumed and additional experiments must be performed so that dense film permeation data can be interpreted in terms of equilibrium surface effects and pore effects. Other objections often raised are the influence of the dense film formation process on the transport, and the assumption of a defect-free uniform film.

An alternative to dense film permeation is the use of sorption measurements [15]. The strength and nature of interactions between two components (permeant, membrane material) can be determined by generating the sorption curve of the permeant for a particular polymer. The experiment involves the recording of the weight gained by the material when the polymer is exposed to a pure vapor phase of the permeant or a pure liquid stream of the permeant. The rate of weight increase is interpreted as the diffusivity of permeant in the membrane material. The maximum amount of permeant that the polymer can adsorb over a long period of time is the equilibrium concentration of permeant. If the sorption behavior for the solute is desired then exposure of the membrane material to a vapor phase will simulate

the conditions for a dilute solute-solvent system. Similarly, using a pure liquid, the system will resemble a concentrated solute-solvent environment. The problem associated with this type of experiment is that only two components of a membrane-solvent-solute system are represented. Therefore the sorption data does not truly represent the membrane separation system.

A variation of the pure component sorption experiments is the classic adsorption experiment. Polymer powder is immersed in a solvent and a solute bath of fixed composition. The change in concentration as the solute is adsorbed onto the surface of the polymer is recorded. This process is carried out for different concentration of solute in the bulk solution. The adsorption isotherm can be generated by plotting the mole fraction decrease (Δx) of n_0 moles of liquid per weight (m) of a solid versus the mole fraction (x) of solute in the bulk solution. The difficulty associated with this experiment is in the measurement of small changes in concentration for dilute solute systems. The nature of the experiment requires large amounts of polymer in order to provide the necessary surface area so that weak interactions can be observed. The batch process involving the wait for the concentration change to reach equilibrium is both tedious and time consuming.

Chromatography has been used as a method of measuring the amount of adsorption by a solid in a liquid system [16]. This experimental method offers the advantages of a continuous process as well as the simulation of the equilibrium conditions present at the membrane-solution interface. Matsuura [17] used the principle of chromatography to interpret the interactions at the membrane-solute-solvent interface. He proposed [18] that the force constants used in the surface potential function as well as the surface excess (Γ) at the interface can be evaluated using a liquid chromatography system. LC data can estimate such parameters as the electrostatic repulsion force constant (A) and Van der Waals attraction force constant (B) as well as the surface excess. Chromatography therefore provides a means of decoupling the influence of the surface from the effect of the pore and pore size. The true nature of the material contribution to membrane separation and transport across the membrane can then be determined.

Chapter 3

Liquid Chromatography (LC)

3.1 Liquid Chromatography : An Introduction

Chromatography is a term applied to all techniques which enable the separation of chemical mixtures by exploiting the phenomenon of differential migration as a solution passes through a column. A carrier fluid containing a mixture is passed over a bed of porous material. Each component of the mixture has its own distinct physical and chemical properties resulting in different rates of migration for each individual element. This idea of different rates of movement for components of a solution through a packing is applicable regardless of the phase of the solution or the nature of the packed bed. Chromatography can be subdivided into gas-solid chromatography, gas-liquid chromatography and liquid-solid chromatography.

The liquid chromatography system consists of a carrier liquid (solvent), various components (solutes) dissolved in the liquid as well as a porous support. There is a distribution of components in the fluid between a mobile and a stationary phase due to the presence of the packing material. This distribution is due to the difference in adsorption potential of the solute and solvent as well as the differences in interaction energies between the mobile and stationary phases.

There is a direct relationship (figure 5) between the physicochemical process in a liquid chromatography system and the actions at the membrane-solution interface. Both systems are concerned with the behavior of a surface-influenced liquid layer.

This layer is known as the stationary phase in LC terms, while for membrane systems the term interfacial layer is used. The mobile phase in a LC system is analogous to the bulk solution of a membrane system. The introduction of a solute in either system results in a concentration difference between the mobile (bulk) phase and stationary (interfacial) phase. This differential concentration results in a retention time difference in the case of a liquid chromatography system, and produces positive and negative concentration gradients at the membrane-solution interface.

Due to the similarities between the two systems, the activities on the surface of a membrane can be obtained by relating the interfacial behavior to quantitative values obtained in a LC system. The nature and strength of the interactions between the solute and the membrane are reflected in the retention time (t_a) of the solute (a) in a liquid chromatography column. A relative scale can be set up to compare the interactions . The result can be interpreted as follows: Suppose the retention time for solute c (t_c) is greater than the retention time for solute d (t_d), this means the polymer has a greater affinity for c than d. Therefore, if the polymer is to be made into a membrane, we can say that the separation process will be based on the rejection of d and the permeation of c. The liquid chromatography data can also provide the means of estimating the surface excess value (Γ) if the area of the solid support is known.

3.2 Solute Retention in LC Systems

The retention time (t_a) describes the time of passage of a solute (a) through any chromatographic column under the influence of the packing [19]. The relationship between the experimentally determined retention time and the distribution of the solute between the mobile phase and stationary phase can be obtained by considering the definition of t_a. This value can be determined by dividing the length of the chromatographic column by the average migration velocity of the solute (v_a) :

$$t_a = \frac{L}{v_a} \tag{14}$$

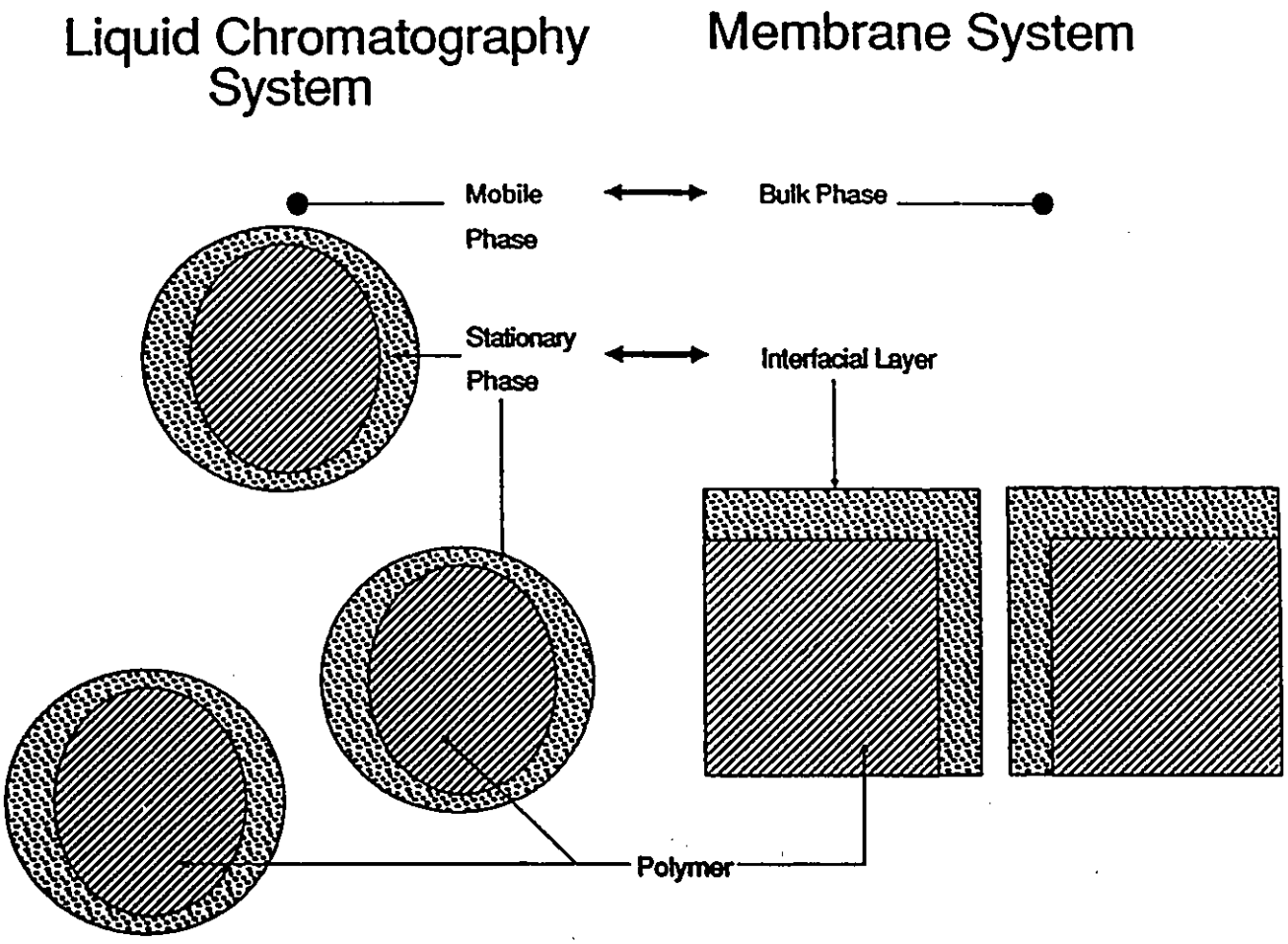

Figure 5: Relationship between a Liquid Chromatography System and a Membrane system

The solute is distributed over a stationary phase and a mobile phase. v_a is determined by the product of the moles of solute in the mobile phase ($q_{a,m}$) over the total moles of solute in both mobile and stationary phases and the velocity of the mobile phase (u) :

$$v_a = (\frac{q_{a,m}}{q_{a,m} + q_{a,s}})u \tag{15}$$

A hold up time (t_0) based on the flow of only the mobile phase over the column can be defined :

$$t_0 = \frac{L}{u} \tag{16}$$

Combining equation (14,15,16) yields

$$t_a = (1 + \frac{q_{a,s}}{q_{a,m}})t_0 \tag{17}$$

This equation relates the retention time to the hold up time. A capacity ratio (k'_a) can be defined as the moles of solute in the stationary phase over the moles of solute in the mobile phase. Equation (17) can be rewritten as :

$$t_a = (1 + k'_a)t_0 \tag{18}$$

The retention time varies inversely as the carrier flow rate (V). An expression for this value, independent of system dimensions, is to characterize retention behaviour in terms of the volume flow between injection of the solute into the column and the emergence of a maximum concentration of the solute at the end of the system [20]. This value is known as the retention volume (V_r); it can be obtained by multiplying the retention time by the volumetric flow rate.

$$V_r = t_a V \tag{19}$$

Equation 18 can be combined with equation 19 so that :

$$V_r = (1 + k'_a)Vt_0 \tag{20}$$

$$= Vt_0 + Vt_0k'_a \tag{21}$$

If $Vt_0 = V_m$, then

$$V_r = V_m + k'_aV_m \tag{22}$$

where :

V_r – Retention volume of the solute

V_m – Volume for the mobile phase

The capacity ratio can be equated to an equilibrium constant (K'_a) as follows [21] :

$$K'_a = \frac{c_{a,s}}{c_{a,m}} \quad (23)$$

$$= \frac{q_{a,s}/V_s}{q_{a,m}/V_m} \quad (24)$$

$$= k'_a(\frac{V_m}{V_s}) \quad (25)$$

where :

$c_{a,m}$ – Solute concentration in the mobile phase

$c_{a,s}$ – Solute concentration in the stationary phase

K'_a – Equilibrium distribution coefficient for the solute between the stationary and mobile phase

V_s – Volume for the stationary phase

Equation 22 can be rewritten in terms of the equilibrium distribution :

$$V_r = V_m + K'_a V_s \quad (26)$$

The degree of retention of a sample is characteristic of the sample and is dependent on the solubility, adsorption, size and degree of ionization of that compound [19]. Equations 18 and 26 establish the fundamental equation of chromatography. The assumption directly linked to this equation is that all substances should actually spend the same length of time in the mobile phase. The difference in the retention time for any solute is due to the residence time in the stationary phase. The result of any chromatography experiments can yield the partition coefficient between the mobile and stationary phase.

Furthermore, if $K'_a > 1$, then the solid substrate is said to preferentially adsorb the solute while for $K'_a < 1$ the interface has a tendency to reject the solute. The distribution coefficient will be dependent on the chemical nature and temperature

of the liquid phase forming the system. In general, the retention volume of a component increases with the change in the distribution coefficient or an increase in the ratio of the stationary to the mobile phase.

3.3 LC data and Surface Interactions

The retention volume of solute a (V_{r_a}) from any chromatography system contains the contribution of the mobile phase (V_m), the stationary phase (V_s) as well as a quantity known as the system dead volume (V_d). The experimental retention volume is the sum of the various contributions :

$$V_{r_a} = V_m + V_d + K'_a V_s \tag{27}$$

The system dead volume can be defined as the volume in a chromatography system which does not contribute to the retention time of the solute due to surface interactions. The system dead volume is the total void space in the chromatography instrument. This includes the volume of the injector, the volume of the capillary lines, as well as the volume of the detector and any connectors.

The values of V_d, V_m, and V_s must be determined in order for a distribution coefficient to be defined. Each of these quantities is extremely difficult to obtain unless certain assumptions are made.

There is an equal probability for any water molecule in a liquid chromatography system to exist in either the mobile phase or in the stationary phase. Therefore, the equilibrium distribution coefficient for water should be one. Deuterium oxide (D_2O) is assumed to be representative of water molecule and therefore should have similar partition behavior. The advantage of D_2O is that it can be detected by a refractometer. The injection of D_2O into the chromatography system represents the introduction of a water molecule from the aqueous component of a solution. The residence volume given by D_2O will be :

$$V_{r_{D_2O}} = V_m + V_d + V_s \tag{28}$$

The assumption that deuterium oxide and water have similar adsorption behavior is quite reasonable. La Mer *et al.* [22] found that the partition coefficient of D_2O

in ice and water was close to unity. Posey and Smith [23] determined that the distribution value was approximately equal to 1.02. Therefore, LC experiments are justified in using D_2O to establish the solvent front.

Another assumption that can be made is the existence of a solute that is not influenced by the stationary phase. A substance can be found such that the solute only stays in the mobile phase of the column: the distribution coefficient for this material by definition will be zero. The retention volume for this substance will be the smallest retention volume of all solutes injected. This value, known as the minimum retention volume, can be defined as the sum of the system dead volume and the volume of the mobile phase :

$$V_{r_{min}} = V_m + V_d \tag{29}$$

Given the previous two assumptions (eq. 28,29). The retention volume of the stationary phase can be obtained :

$$V_s = V_{r_{D_2O}} - V_{r_{min}} \tag{30}$$

and

$$K'_a V_s = V_{r_a} - V_{r_{min}} \tag{31}$$

therefore, the distribution coefficient can be calculated by combining equations (30,31).

$$K'_a = \frac{(V_{r_a} - V_{r_{min}})}{(V_{r_{D_2O}} - V_{r_{min}})} \tag{32}$$

The retention volume of the stationary phase can also provide the interfacial layer thickness (Ti) of the stationary phase if the area of the column packing is known.

$$T_i = \frac{V_s}{Area} \tag{33}$$

The surface excess for a distance T_i from the interface is the concentration difference between the bulk ($c_{a,b}$) and the interface ($c_{a,i}$).

$$\frac{\Gamma}{T_i} = c_{a,i} - c_{a,b} \tag{34}$$

in ice and water was close to unity. Posey and Smith [23] determined that the distribution value was approximately equal to 1.02. Therefore, LC experiments are justified in using D_2O to establish the solvent front.

Another assumption that can be made is the existence of a solute that is not influenced by the stationary phase. A substance can be found such that the solute only stays in the mobile phase of the column: the distribution coefficient for this material by definition will be zero. The retention volume for this substance will be the smallest retention volume of all solutes injected. This value, known as the minimum retention volume, can be defined as the sum of the system dead volume and the volume of the mobile phase :

$$V_{r_{min}} = V_m + V_d \tag{29}$$

Given the previous two assumptions (eq. 28,29). The retention volume of the stationary phase can be obtained :

$$V_s = V_{r_{D_2O}} - V_{r_{min}} \tag{30}$$

and

$$K'_a V_s = V_{r_a} - V_{r_{min}} \tag{31}$$

therefore, the distribution coefficient can be calculated by combining equations (30,31).

$$K'_a = \frac{(V_{r_a} - V_{r_{min}})}{(V_{r_{D_2O}} - V_{r_{min}})} \tag{32}$$

The retention volume of the stationary phase can also provide the interfacial layer thickness (Ti) of the stationary phase if the area of the column packing is known.

$$T_i = \frac{V_s}{Area} \tag{33}$$

The surface excess for a distance T_i from the interface is the concentration difference between the bulk ($c_{a,b}$) and the interface ($c_{a,i}$).

$$\frac{\Gamma}{T_i} = c_{a,i} - c_{a,b} \tag{34}$$

The average concentration of the interfacial layer can be related to the bulk concentration by a equilibrium constant ($K_{a,i}$). Therefore :

$$\frac{\Gamma}{T_i} = c_{a,b}K_{a,i} - c_{a,b} \quad (35)$$

$$= (K_{a,i} - 1)c_{a,b} \quad (36)$$

If $K_{a,i} = K'_a$, then

$$\frac{\Gamma}{T_i} = (K'_a - 1)c_{a,b} \quad (37)$$

or

$$K'_a = \frac{\Gamma}{T_i c_{a,b}} + 1 \quad (38)$$

The interfacial concentration is dependent on the distance from the pore wall. The surface excess can be calculated as a sum of three integrals. In an aqueous system, there is no solution when the distance is less then the radius of the water molecule (D_w). The distance from D_w to the radius of a solute molecule (D_s) (ie. $D_w < d < D_s$) has an interfacial concentration of zero. This concentration is zero because by definition the center of the solute molecule only exists when the distance is greater than the radius. The interfacial concentration can be related to the bulk concentration by means of the Maxwell-Boltzmann distribution (see equation 11) for distance greater than the radius of the solute molecule (ie. $D_s < d < \infty$). The surface excess then can be evaluated as follows :

$$\Gamma = \int_{D_w}^{D_s} (0 - c_{a,b})d(d) + \int_{D_s}^{\infty} |(c_{a,b}\exp(-\phi(d)) - c_{a,b})|\, d(d) \quad (39)$$

$$= \left((D_w - D_s) + \int_{D_s}^{\infty} |(\exp(-\phi(d)) - 1)|\, d(d)\right) c_{a,b} \quad (40)$$

Combining with equation 40 :

$$K'_a = \frac{(D_w - D_s) + \int_{D_s}^{\infty} |(\exp(-\phi(d)) - 1)|\, d(d)}{T_i} + 1 \quad (41)$$

$$= \frac{\int_{D_w}^{\infty} |(\exp(-\phi(d)) - 1)|\, d(d)}{T_i} + 1 \quad (42)$$

The chromatography data can be used to generate potential functions for the membrane solute interactions if the partition coefficient generated by the LC is analogous to the equilibrium distribution at the membrane solution.

3.4 Surface Area Measurements

The surface area of the LC column is measured using gas chromatography [24,25,26]. The water adsorption isotherm for the column is generated according to the following equations :

$$p = \frac{nRT}{V_{gas}} \tag{43}$$

and

$$N_a = \frac{nS_a}{m_p S_{locus}} \tag{44}$$

where :

- S_{locus} – Area obtain from the locus of peak maxima
- S_a – Area under the peak
- p – Partial pressure of the water vapor
- n – Moles of water injected
- V_{gas} – Volume of gas that pass through the column
- N_a – Number of moles of water adsorbed
- m_p – Mass of Polymer

The values obtained from gas chromatography data can best be shown in figure 6.

The Brunauer, Emmett, and Teller (BET) equation can be applied to the adsorption isotherm [27] assuming mono-layer coverage of water on the polymer. The adsorption data is plotted in the form $P/(N_a(P\text{-}P_{sat}))$ vs. P/P_{sat}. A linear regression is performed to obtain the slope (m) and intercept (b) in terms of a constant (C) and a the mono-layer capacity of water on the polymer (n_{sm}).

$$m = \frac{C-1}{Cn_{sm}} \tag{45}$$

$$b = \frac{1}{Cn_{sm}} \tag{46}$$

therefore :

$$n_{sm} = (m+b)^{-1} \tag{47}$$

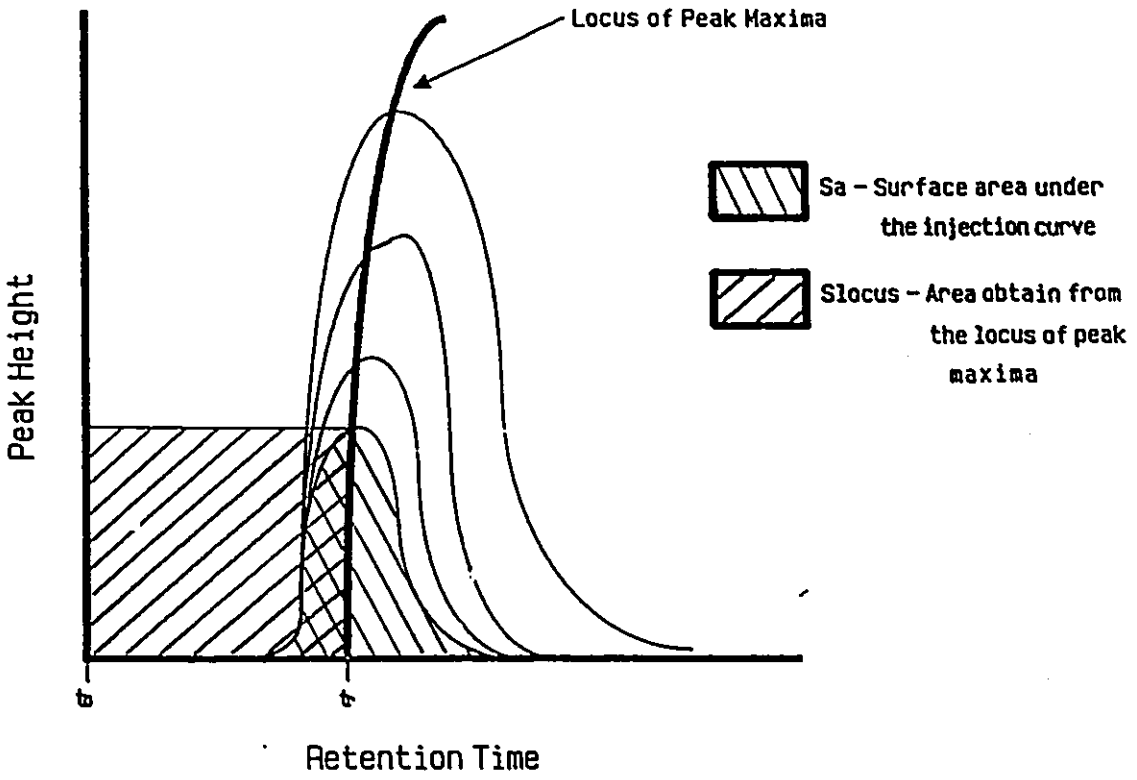

Figure 6: Gas Chromatography data

The surface area (S_A) can be calculated once the number of water molecules adsorbed onto the polymer surface (n_{sm}) is known.

$$S_A = \frac{n_{sm}}{M_w} \cdot N \cdot A_m \times 10^{-20} \tag{48}$$

A_m – Molecular cross-sectional area of the adsorbate (water)

N – Avogadro's Constant (6.02×10^{23} molecules per mole)

M_w – Molecular weight of water

The area of the water molecule (A_m) was taken to be 14.8 A^2 [28].

Chapter 4

Experimental Methods

4.1 Production of Chromatography Packing

A preliminary investigation was conducted to determine the best way to make a suitable chromatography column packing from the test polymer. The size of the particle, its porosity, and the nature of its surface are important factors that determine its effectiveness when packed in a chromatography column. An ideal particle would have surface properties similar to that of a cast membrane. Three different methods of preparation were investigated : direct crushing of the polymer, dilute precipation and spraying.

4.1.1 Direct Physical Crushing

Commercial polysulfone polymer is available in the form of hard cylindrical pellets. They are two to three millimeters in length and one half millimeter in diameter. In these experiments, Udel was obtained from Amoco; Victrex was purchased from ICI America Inc.; and Radel was acquired from Union Carbide. The size of the pellets must be reduced before they can be used as chromatography packing.

The first method used to break the material down involved a combination of thermal shock and mechanical force. The material was first immersed in liquid nitrogen to increase the brittleness of the polymer. The cold polymer was then put

into a Waring blender. The action of the blade in the blender caused the pellets to spin at great velocity inside a stainless steel container. The polysulfone was crushed against the wall of the blender due to high speed impaction. High speed collision combined with the mechanical cutting actions of the Warring blender blades resulted in a size reduction of the particles. The particles were then sieved with Tyler sieves (400 Mesh and 270 Mesh) to obtain the desired particle diameter of 38-53 μm.

4.1.2 Dilute Precipitation

The second method of size reduction of the polymer involved the precipitation from a dilute polymer solution and the mechanical break down of the resulting precipitate. A solution comprising of 10% polymer and 90% N-methyl-pyrrolidone (NMP) was precipitated directly into a Warring blender containing water. NMP is a solvent for the polymer and is extremely soluble in water. Water cannot dissolve the polymer. Mixing water, solvent and polymer together results in the polymer coming out of solution and forming a solid. Low polymer concentration minimized the chain entanglement of the polymer while in solution. A rapid mixing of water during precipitation reduced the possibility of aggregation of the polymer chains. The two effects together produced a very open precipitating polymer structure. The polymer structure was further fragmented by the mechanical action of the Warring blender blades. The mixture of water and precipitated polymer was later sieved. The desired fraction in the range of 38-53 μm was recovered. This fraction was then dried in a convention oven.

4.1.3 Spraying

The third method of producing chromatography packing involved the principle of spray drying. Polymer particles were made by spraying a fine mist of polymer solution into an open column; the droplets of solution were then allowed to precipitate into water. The spraying equipment (figure 7) consisted of : an atomizing source (air), a pressurized feed (polymer solution), an appropriate nozzle, a container and a water bath at the end of the column.

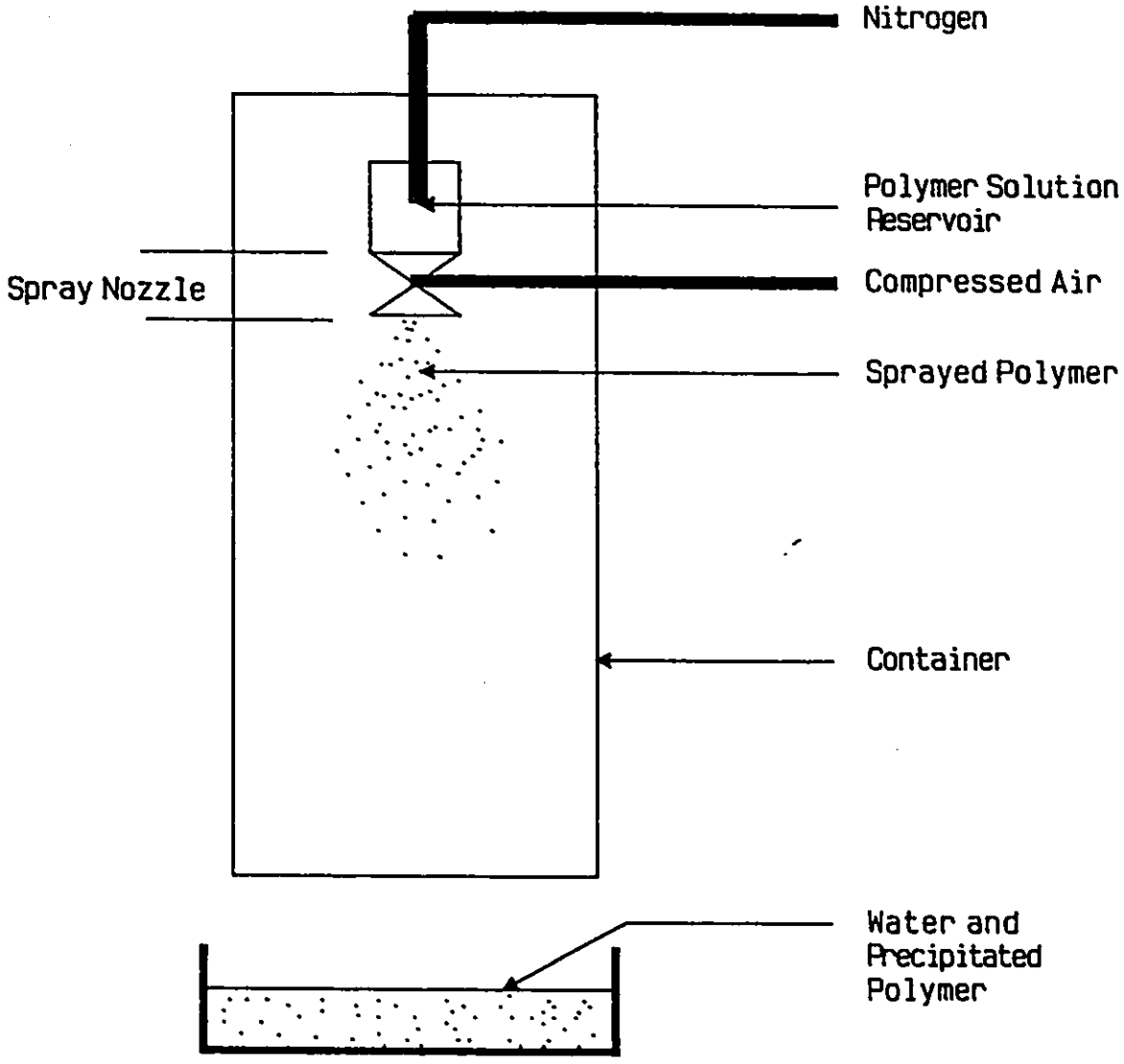

Figure 7: The spraying column

The fine mist of polymer solution droplets was produced by a two fluid-nozzle. This nozzle was based on the principle that a liquid stream (polymer solution) could be broken down into small droplets due to impact with a high velocity gas stream (air). A small nozzle was developed that could handle the small volume of polymer solution as well as produce the size of the particles required. The final design (figure 8) consisted of a series of 3/16" stainless steel Swagelok fittings and a 22-gauge hypodermic needle.

The feed was fifteen to twenty weight percent polysulfone dissolved in NMP. This feed was stored in a stainless steel container and was forced through the 22 gauge hypodermic needle using nitrogen at 400 PSI. At the exit of the needle, the solution was broken up into small droplets by a high velocity compressed air at a pressure of 100 PSI.

The sprayed polymer was in the form of small droplets containing both NMP and polymer. These droplets were allowed to fall into a water bath located at the bottom of a six meter open ended column. The fall residence time of 10-20 seconds allowed for evaporation of some of the solvents and allowed the droplets to maintain tight skin surface so that the particle could maintain a spherical shape. Finally, immersion of the droplets in water resulted in the precipitation of the polymer. Tyler sieves were utilized to obtain the desired particle range (38-53 μm). The recovered powder was dried in a convection oven and was ready for packing.

4.1.4 Packing the Chromatography Column

The column was initially packed in a dry state. A 60 cm (1/8" OD. - 0.020 Wall 304SS) chromatography column was first weighed. A funnel containing 5 grams of dried polymer powder (38-53 μm) was then attached to the inlet of the column. This system was subjected to a constant vibration for ten hours. The column was re-weighed and then tested in the LC system.

A wet packing method, involving high pressure packing of a fine suspension of particles, was also tried. A Shandon column slurry packing instrument obtained from Chromatography Sciences Company (CSC) was purchased and tested.

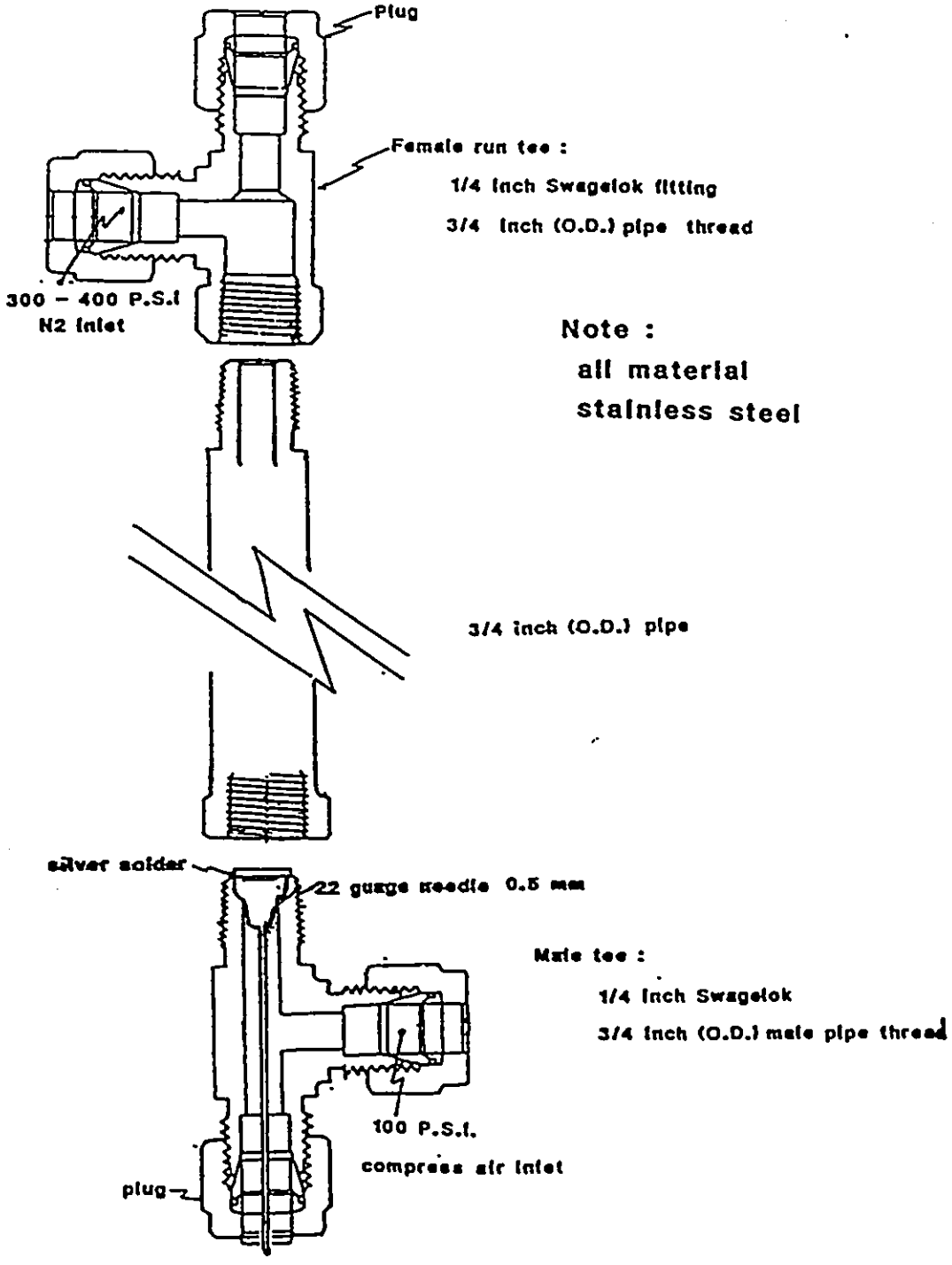

Figure 8: The spraying nozzle

4.2 Liquid Chromatography Apparatus

A Waters Associate liquid chromatograph (model ALC202) fitted with a R4000 refractometer was used in this work. The refractometer signal was fed to a Perkin-Elmer Sigma 1000 integrator. The integrator signal was down-loaded directly into an IBM compatible micro-computer (IBM-XT). The raw data was stored on 5 $\frac{1}{4}''$ floppy diskette. The time taken for the appearance of a maximum recorded response after each injection was defined as the retention time of the solute. The system setup is given in figure 9. The column and the refractometer were both cooled by a recirculating water bath so that the system temperature did not fluctuate by more than $\pm$ 2 degrees from the control temperature of 25°C.

The solvent (water) was obtained from a Millipore ultrapure water system in order to ensure the water purity. The system produced water of 18 MΩ of resistance and particulate contaminates were removed by passing the water through a 0.22 μm filter. Water was degased by boiling the water for several minutes.

A one weight percent water solution was made of all the solutes that were tested. Ten μl of this solute was injected by hand directly into the column using a 50 μl Hamilton syringe. The water flow rate was set at 0.3 cm^3/min.

4.3 Gas Chromatography Equipment

The experimental setup used to obtain the specific surface area of the chromatography column was similar to that described by Matsuura *et al.* [29]. A Tracor (Model 160) gas chromatograph equipped with a thermal conductivity meter was used. The signal from this detector was fed to a Perkin-Elmer Sigma 1000 integrating station. The integrator data was transfer to an IBM-XT. The system set-up is summarized in figure 10. Again, the original data was stored on a floppy diskette. The data was analyzed to obtain the total area under the elution curve as well as the retention time. The water vapor adsorption isotherm of the chromatography column was obtained from calculations involving the area under the elution curve, the retention time and the area of the locus of the peak maximum (section 3.4).

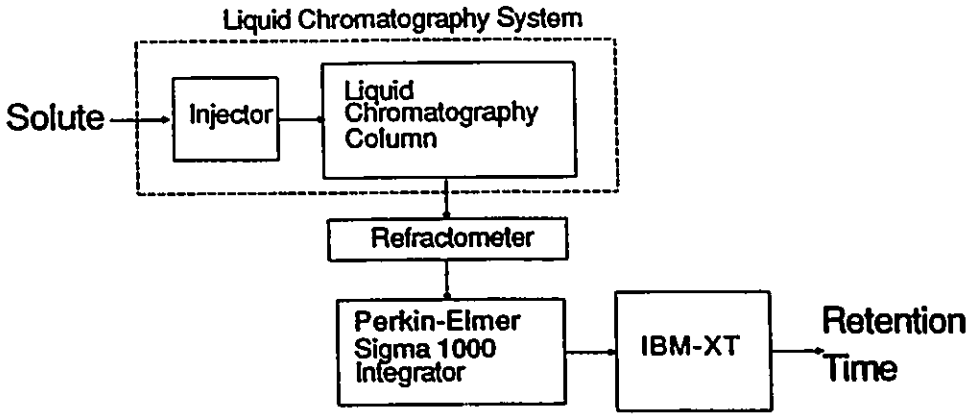

Figure 9: Liquid Chromatography System set-up

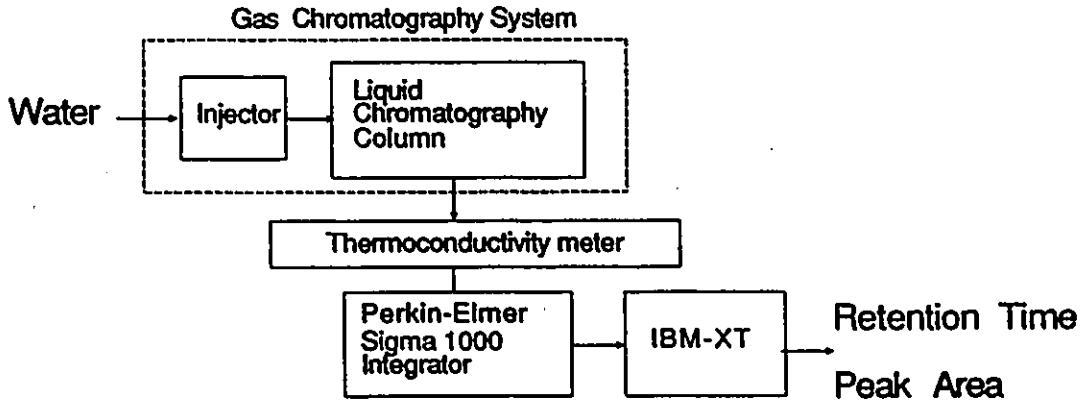

Figure 10: Gas Chromatography System set-up

The liquid chromatography column was connected to the gas chromatography system after the retention time for all chosen solutes were obtained. This column was left in the gas chromatography system at 50°C to dry with helium gas passing through the column. The operating temperature of the system was 80°C. The carrier gas was helium and the flow rate was set at 10 cm^3/min. Air was injected into the system to determine the dead time. Different volumes of water were injected into the system using a microliter syringe. The maximum volume of water required to reach saturation was usually 25 μL.

4.4 Choice of Solutes

There are a great number of chemicals that can be used as solutes to study surface interactions of a polymer. The solutes involved in the current experiments are limited with the following considerations :

- The chemicals must be readily available .
- The solute poses a potential separation problem in aqueous systems. There was also a special emphasis on the eventual application in the area of Biotechnology.
- The targeted material have desirable properties that point to a specific action at an interface.

Table 1 is a list of the inorganic materials that were tested. Salts of different ionic radii and valence states were chosen [13]. The information concerning the various salts is important in the overall area of desalination and the production of ultrapure water. The table also contains a selection of carbohydrates tested. Each sugar has a different molecular weight and size [13]. They are important in the field of Biotechnology because they are commonly used as starting materials. Metabolites and other desirable products have to be recovered from the sugar substrate after biological reactions.

Table 1 also contains a series of polyethylene glycols (PEG). The molecular weights of these polymers range from the pure ethylene glycol repeat unit to a

molecular weight of thirty-five thousand (PEG 3500). They were chosen because they are often used in the characterization of ultrafiltration membranes and nanofiltration membranes. Membrane solute interaction parameters must be generated so that future work on characterization of polysulfone and modified polysulfone can make use of the Surface Force Pore Flow (SFPF) model. The table also lists a family of alcohols . The chain length as well as the effect of branching are represented. Alcohols are especially important in the field of fermentation. Other solutes included in the screening study were a group of low molecular weight organic solutes that were readily available. This group included amines of different chain length as well as small fatty acids. Together they provided some insight into the nature of the polymer material due to the difference in the functional group.

Special care was used to maintain the purity of the solutes. Whenever possible, analytical standards for the chemicals were obtained. The series of inorganic salts were obtained from Aldrich Chemical Company, Inc. . Organic chemicals such as the PEG were purchased from Fluka Chemical Corp. . Ultrapure samples of alcohols, amines and fatty acids that were considered as chromatography standard were available from Polyscience Inc. .

Monovalent		
LiCl	NaCl	KCl
RbCl	NaF	NaBr
NaI	KBr	CsBr
NH_4Cl		
Divalent		
$MgCl_2$	$SrCl_2$	$BaCl_2$
$CaCl_2$		Potassium biphthalate
Sugars		
Sucrose	D-Sorbitol	Erythritol
Maltose	Xylitol	D-Glucose
Fructose	Raffinose	
Low Molecular Weight Polymers		
PAA6000	Ethylene glycol	PEG 200
PEG 300	PEG 400	PEG 600
PEG 1000	PEG 1530	PEG 2000
PEG 3000	PEG 4000	PEG 6000
PEG 12000	PEG 35000	
Alcohols		
Methanol	1-Butanol	1-Pentanol
Ethanol	2-Butanol	2-Pentanol
1-Propanol	2-Methyl-1-propanol	3-Pentanol
2-Propanol	2-Methyl-2-propanol	2-Methyl-1-butanol
3-Methyl-1-butanol	2-Methyl-2-butanol	
Acetates		
Methyl acetate	Ethyl acetate	
Amines		
n-Butylamine	iso-Butylamine	sec- Butylamine
tert-Butylamine	n-Amylamine	iso-Amylamine
n-Hexaylamine	Benzlamine	n-Heptylamine
Fatty Acids		
Propanoic acid	Butanic acid	Pentanoic acid
Others		
Ether	Glycerol	D_2O
Methyl-ethyl-ketone	Nitromethane	N,N-Dimethyl aniline

Table 1: List of Solutes Tested

Chapter 5

Results

5.1 LC Column Packing Studies

An appropriate means of producing packing particles for the chromatography column was determined before any surface interaction data were obtained. The types of material made from the three different preparation methods described in sections 4.1.1, 4.1.2,and 4.1.3 were compared both physically and in terms of liquid chromatography performance.

	Production Method		
Polymer	Crushed	Precipitated	Spray
Udel	1.83	.75	1.29
Radel	1.72	.81	1.04
Victrex	1.65	.82	.88

Table 2: Comparison of Bulk Density of Polymers (g/cm^3)

An optical microscope fitted with a 35mm camera was used to take pictures of particles obtained from various production methods (Figures 11,12,13). Figure 11 shows particles made from direct crushing. The particles produced using

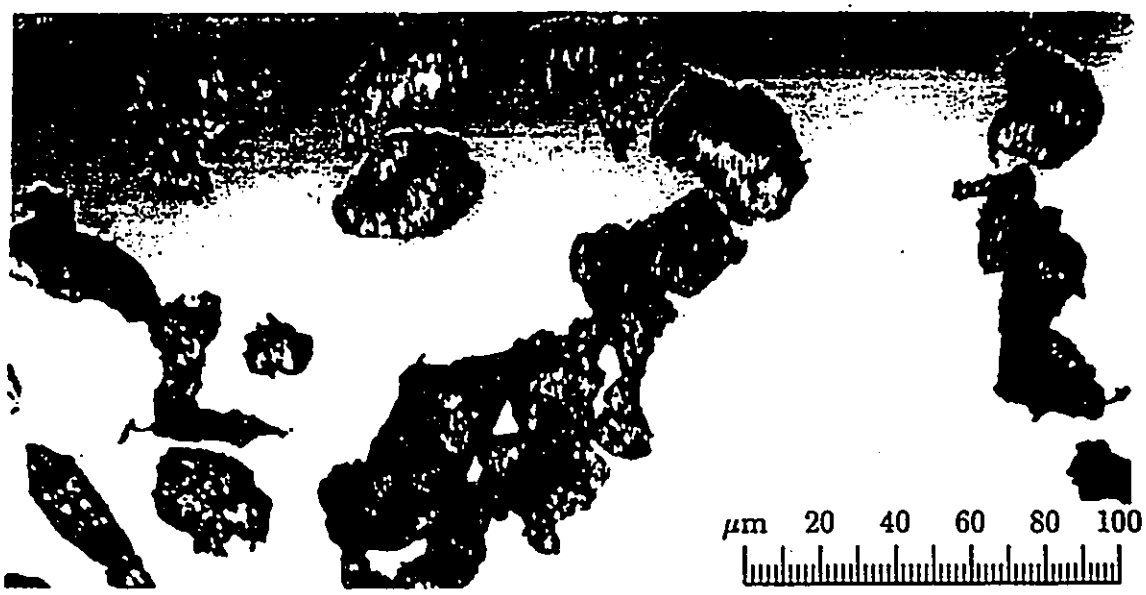

Figure 11: Particles produced from Direct Crushing (magnified 2000 times)

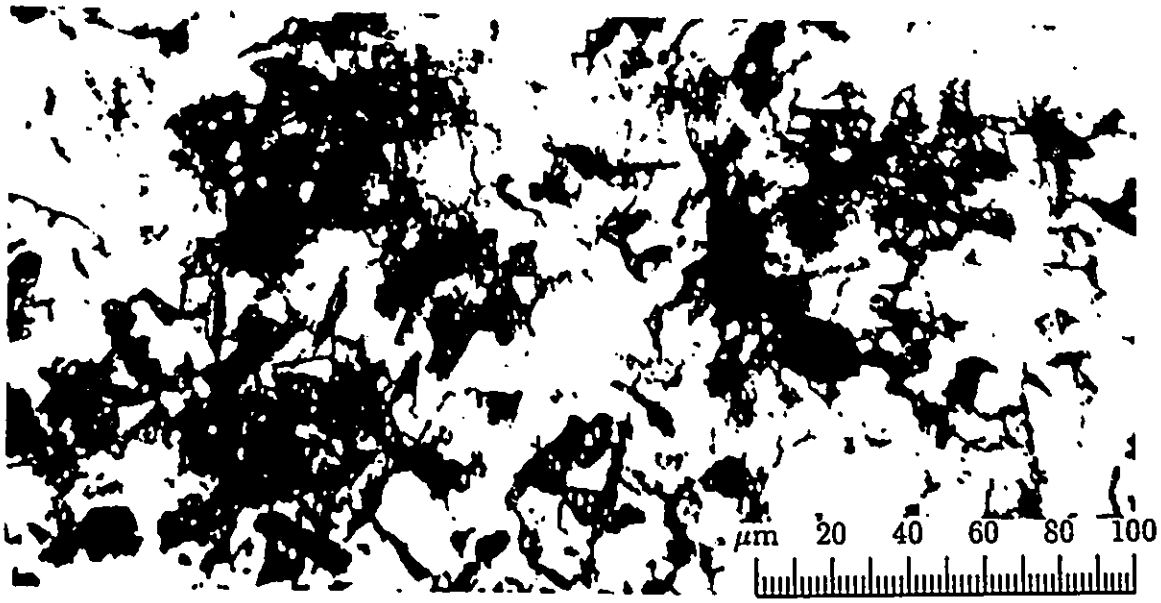

Figure 12: Particles produced from Dilute Precipitation (magnified 2000 times)

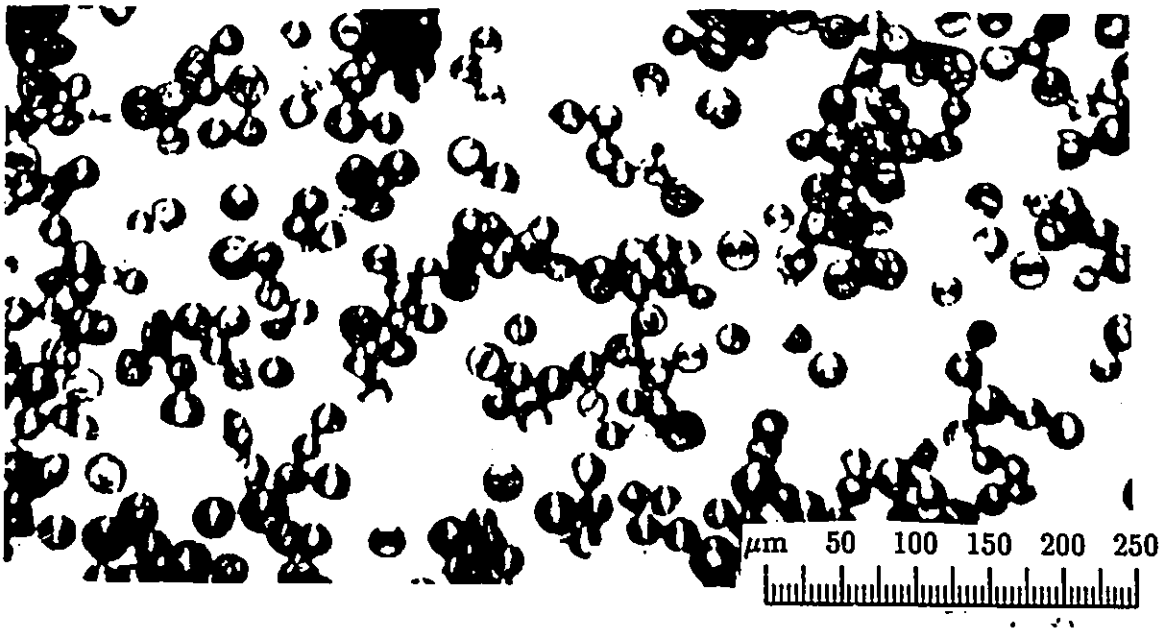

Figure 13: Particles produced from Spraying(magnified1000 times)

this method were solid irregular blocks. Figure 12 is a picture of particles obtained from precipitation of a dilute polymer solution. The particles made using this method appeared fibrous . Figure 13 shows the product from the sprayer. The photograph shows regularly shaped spherical particles. There are advantages to using the sprayed material in liquid chromatography. Spherical packing particles have higher permeability than irregular shaped particles [20].

There were other physical differences between particles made from the different production methods. The particles made by precipitation had a much lower bulk density than those made by direct crushing or spraying (Table 2). This difference could be explained by the fibrous open structure of the precipitated polymer which resulted in less compact packing and consequently lower bulk density.

The materials were packed into chromatography columns and tested in the LC system. Table 3 compares the retention times generated by the three different types of packing. The column packed with crushed polymer pellets did not show any retention time difference between inorganics, carbohydrates and alcohols. The column packed with precipitated powder showed definite separation between different class of solutes. However, the peak shapes of the chromatograms were broad

and unsymmetrical. This indicated the presence of diffusional effects in the column. This result, combined with the previous observation of significantly lower bulk density, led to the conclusion that there were large void spaces in the packed column. Therefore, this was not a suitable method for producing chromatography packing. This conclusion was further justified when sprayed particle packing had retention time difference between members in the alcohol series while there were no such difference for columns packed from physically crushed particles.

	Udel			Radel		Victrex	
Solute	Crushed	Precipitated	Sprayed	Crushed	Sprayed	Crushed	Sprayed
NaCl	5.30	6.43	6.54	5.30	7.62	5.40	7.35
Methanol	5.28	6.47	6.90	5.48	8.21	5.50	7.72
Ethanol	5.32	7.10	8.62	5.42	9.59	5.27	8.62
2-Propanol	5.00	6.45	11.16	5.32	12.42	5.42	10.62
tert-Butanol	4.97	6.97	16.38	5.38	35.94	5.33	19.72
Pentanol	5.42	7.20	-	5.30	-	5.30	26.44
Sucrose	5.27	6.42	6.43	5.25	7.78	5.30	7.20
Glucose	4.98	6.38	6.47	5.34	7.63	5.28	7.43
D_2O	5.10	6.43	6.72	5.35	7.66	5.35	7.21
Ethylene glycol	-	-	6.67	5.33	7.78	5.28	7.26
PEG 200	-	7.117	7.35	5.23	8.63	5.40	7.79
PEG 1000	-	6.77	-	5.80	-	5.38	7.45
PEG 3500	5.25	14.38	-	5.73	-	5.38	-

Table 3: Comparision of Retention Times (Minutes) for Different Production Methods

No noticeable difference in terms of LC performance was obtained by the two column packing methods. The slurry packing method proved to be more troublesome than dry packing. Polysulfone particles are hydrophobic and are difficult to disperse in water. The slurry packing method required the particles to stay in suspension long enough so that the slurry could be effectively filtered through the chromatography support. Also, the particle size ranges for the column were too large to take full advantage of the benefits provided by the slurry packing apparatus.

5.2 LC Retention Time Data

Tables 4 to 8 summarize the average retention time and the average retention volume data for the five types of polysulfones tested. The polysulfones included are three commercially available polymer - Udel, Victrex and Radel; as well as two modified polysulfone - carboxylated polysulfone (CPS) and trimethylsilyl polysulfone (TMS). At least three retention time measurements were made for each solute and the average retention times was reported. The variance for each solute retention time was calculated and a 95% confidence interval (95% C.I.) was obtained. This confidence interval ranged from 2 to 10 percent of the average value. Comparison of solute retention time differences must take into account the difference in average retention time as well as the region where this average value could be found (ie.the 95% C.I.).

In the series of inorganic salts and carbohydates, there were only small differences in the average retention time between members of the same series. No definite conclusion could be drawn from the difference in retention time between these solutes when the confidence interval was taken into consideration. For the inorganic salt series, the effect of ionic size could not be differentiated using the present liquid chromatography system. The whole series of sugars from glucose to sucrose yielded similar retention times. The effect of different molecular weights of sugars on chromatography data cannot be determined using the present chromatography system. The high level of uncertainty in retention times can be attributed to fluctuating carrier flow rate and peak broadening diffusional effects.

The retention times of different groups of substances can be compared. In general, different series of solutes have the following retention time tendency for all the polysulfones tested :

$$\text{inorganics,carbohydrates} < D_2O < \text{amines} < \text{alcohol,PEG's.}$$

This corresponds to the observation of Matsuura *et al.*[13] for cellulose acetate and Victrex polysulfone polymers.

Tables 4 to 8 contain only solutes that have a clearly identifiable retention time. All the solutes listed in table 1 were tested for all five polymers. Some of the solutes

were not tabulated because they produced inconsistent chromatography peaks or were irreversibly adsorbed on to the column. Such solutes varied for different polymer columns, due to the difference in physicochemical nature of different polymer packing.

Solutes eluted with a skewed peak shape and tailing baselines provide an indication of the strength of interactions in between the solute and the solid support. Unfortunately, the chromatography data generated by such solutes could not be handled by the present method for determining the retention time. The solutes that generated such data include branch alcohols (2-Methyl-2-butanol) and some amines (benzlamine). These solutes were omitted from further analysis.

Some solutes tested were injected into the column but had no peaks. These solutes were irreversibly adsorbed onto the packing material and could not be eluted out of the column. These solutes included polyethylene glycols with a molecular weight greater than 1530 (ie. PEG 1530 - PEG 35000). Substances which were extremely hydrophobic such as pentanol, methyl-ethyl ketones and ethers did not yield a retention time. Aromatic compounds such as aniline and benzene also bound to the polymer. Solutes that were considered possible to be retained irreversibly were tested last so that this irreversible adsorption would not affect the retention time of the other solute.

Solutes	Average Retention time (minutes)	95% C.I.	Average Retention Volume (cm^3)
LiCl	6.44	.02	1.93
NaCl	6.54	.35	1.96
KCl	6.51	.21	1.95
RbCl	6.63	.44	1.99
NaF	6.54	.12	1.96
NaCl	6.54	.35	1.96
NaBr	6.77	.46	2.03
NaI	6.56	.61	1.97
KBr	6.53	.06	1.96
CsBr	6.54	.10	1.96
$MgCl_2$	6.50	.21	1.95
$CaCl_2$	6.55	.07	1.97
$SrCl_2$	6.84	1.07	2.05
$BaCl_2$	6.64	.83	1.99
NH_4Cl	6.44	.27	1.93
Kbiphthalate	6.49	.96	1.95
Sucrose	6.43	.48	1.93
Maltose	6.54	.10	1.96
Fructose	7.01	1.33	2.10
D-Sorbitol	6.47	.07	1.94
Xylitol	6.69	.78	2.01
Raffinose	6.98	.47	2.10
Erthylitol	6.46	.06	1.94
D-Glucose	6.47	.14	1.94
PAA6000	5.33	1.04	1.60
Ethylene glycol	6.67	.27	2.00
PEG 200	7.35	.17	2.21
PEG 300	9.16	.34	2.75
PEG 400	16.01	9.12	4.80
Methanol	6.90	.20	2.07
Ethanol	8.62	.45	2.59
1-Propanol	13.97	1.41	4.19
2-Propanol	11.16	1.54	3.35
2-Butanol	27.67	-	-
2-Methyl-1-propanol	16.38	2.20	4.91
2-Methyl-2-propanol	27.32	.15	2.20
2-Methyl-2-butanol	8.78	.91	2.63
n-Butylamine	6.48	-	1.93
iso-Butylamine	5.56	3.13	1.67
sec-Butylamine	5.13	.38	1.54
tert-Butylamine	6.74	7.35	2.02
n-Amylamine	4.64	1.08	1.39
iso-Amylamine	4.50	-	1.35
n-Hexylamine	5.08	-	1.52
Benzylamine	5.67	-	1.70
Propanoic Acid	15.46	4.93	4.64
Butanoic Acid	7.53	-	2.26
Glycerol	6.52	.02	1.96
D_2O	6.72	.09	2.02

Table 4: Retention Data for Udel Polysulfone

Solutes	Average Retention time (minutes)	95% C.I.	Average Retention Volume (cm^3)
LiCl	7.71	.73	2.31
NaCl	7.62	.15	2.29
KCl	7.66	.05	2.30
RbCl	7.66	.89	2.30
NaF	7.97	1.79	2.39
NaBr	7.85	1.16	2.35
NaI	7.58	.37	2.27
KBr	7.54	.27	2.26
CsBr	7.85	1.09	2.36
$MgCl_2$	7.42	.22	2.23
$CaCl_2$	7.73	.58	2.32
$SrCl_2$	7.61	1.49	2.28
$BaCl_2$	7.88	.44	2.37
NH_4Cl	7.59	.42	2.28
Kbiphthalate	9.02	2.37	2.71
Sucrose	7.78	.29	2.33
Maltose	7.73	.39	2.32
Fructose	7.76	.06	2.33
D-Sorbitol	7.65	.35	2.30
Xylitol	7.71	.58	2.31
Raffinose	7.94	.09	2.38
Erthylitol	7.79	.10	2.34
D-Glucose	7.63	.39	2.29
PAA 6000	7.28	.90	2.18
Ethylene glycol	7.78	.40	2.34
PEG 200	8.63	.20	2.59
PEG 300	10.77	.51	3.23
PEG 400	25.20	.65	7.56
PEG 600	7.80	.56	2.34
Methanol	8.21	.85	2.46
Ethanol	9.59	.73	2.88
1-Propanol	16.37	2.39	4.91
2-Propanol	12.42	.50	3.73
1-Butanol	25.61	4.64	7.68
2-Methyl-1-propanol	35.94	12.32	10.78
2-Methyl-2-propanol	8.54	.87	2.56
Methyl acetate	9.79	.10	2.94
Ethyl acetate	9.19	.79	2.76
n-Butylamine	39.29	12.91	11.79
iso-Butylamine	23.21	4.46	6.96
sec-Butylamine	17.31	11.28	5.19
Propanoic Acid	16.74	.31	5.02
Butanoic Acid	50.96	6.83	15.29
D_2O	7.66	.28	2.30
Glycerol	7.68	.25	2.30

Table 5: Retention Data for Radel Polysulfone

Solutes	Average Retention time (minutes)	95% C.I.	Average Retention Volume (cm^3)
LiCl	7.27	.84	2.18
NaCl	7.35	.97	2.21
KCl	7.10	.44	2.13
RbCl	7.27	.13	2.18
NaF	7.32	.04	2.20
NaBr	7.12	.27	2.14
NaI	7.49	.50	2.25
KBr	7.01	1.73	2.10
CsBr	7.06	.66	2.12
$MgCl_2$	6.71	.98	2.01
$CaCl_2$	6.99	1.35	2.10
$SrCl_2$	7.04	1.77	2.11
$BaCl_2$	7.31	.23	2.19
NH_4Cl	7.06	1.82	2.12
Kbiphthalate	8.02	1.69	2.40
Sucrose	7.20	.50	2.16
Maltose	7.36	.75	2.21
Fructose	7.33	.85	2.20
D-Sorbitol	7.45	.50	2.24
Xylitol	7.30	.35	2.19
Raffinose	7.47	.42	2.24
Erthylitol	7.92	1.83	2.38
D-Glucose	7.43	.36	2.23
PAA6000	6.28	.98	1.89
Ethylene glycol	7.26	.46	2.18
PEG 200	7.79	.48	2.34
PEG 300	8.49	.58	2.55
PEG 400	10.94	2.67	3.28
PEG 600	22.50	6.41	6.75
PEG 1000	7.45	1.18	2.23
PEG 1530	7.20	.54	2.16
PEG 2000	6.28	.59	1.88
Methanol	7.72	.54	2.32
Ethanol	8.62	2.06	2.59
1-Propanol	13.67	1.04	4.10
2-Propanol	10.62	.69	3.19
1-Butanol	35.61	3.06	10.68
2-Butanol	20.17	2.62	6.05
2-Methyl-1-propanol	19.74	1.27	5.92
2-Methyl-2-propanol	7.54	.87	2.26
1-Pentanol	26.44	2.50	7.93
2-Pentanol	46.64	1.66	13.99
3-Methyl-1-butanol	7.18	-	2.15
2-Methyl-2-butanol	8.73	-	2.62
Methyl acetate	7.09	.34	2.13
Ethyl acetate	7.74	.58	2.32
n-Butylamine	17.83	-	5.439
iso-Butylamine	12.65	-	3.795
sec-Butylamine	16.82	-	5.046
tert-Butylamine	9.59	-	2.88
n-Amylamine	59.21	-	17.76
iso-Amylamine	27.24	-	8.17
n-Hexylamine	74.53	-	22.36
Propanoic Acid	17.61	-	5.28
D_2O	7.21	.63	2.16
Glycerol	7.74	1.60	2.32

Table 6: Retention Data for Victrex Polysulfone

Solutes	Average Retention time (minutes)	95% C.I	Average Retention Volume (cm^3)
LiCl	5.37	.67	1.61
NaCl	5.39	.64	1.62
KCl	5.49	.17	1.65
RbCl	5.39	.83	1.62
NaF	7.34	.48	2.20
NaBr	5.74	.83	1.72
NaI	5.44	.92	1.63
KBr	5.30	.04	1.59
CsBr	5.90	1.85	1.77
$MgCl_2$	5.39	.25	1.62
$CaCl_2$	5.38	.08	1.61
$BaCl_2$	5.25	.58	1.58
$SrCl_2$	5.26	.11	1.58
NH_4Cl	5.63	.50	1.69
Kbiphthalate	5.35	.12	1.61
Sucrose	5.64	.09	1.69
Maltose	5.71	.59	1.71
Fructose	5.78	.08	1.73
D-Sorbitol	5.92	.15	1.78
Xylitol	6.16	.95	1.85
Raffinose	5.63	.04	1.69
Erthylitol	5.78	.73	1.73
D-Glucose	5.63	.83	1.69
PAA 6000	4.00	.07	1.20
Ethylene glycol	5.79	.10	1.74
PEG 200	7.93	.80	2.38
PEG 300	9.59	.02	2.88
PEG 400	14.11	2.97	4.23
PEG 600	28.60	1.41	8.58
PEG 1000	5.28	.19	1.59
PEG 1530	5.05	.04	1.51
Methanol	6.48	.50	1.95
Ethanol	8.89	.13	2.67
1-Propanol	17.85	3.15	5.36
2-Propanol	14.56	5.84	4.37
1-Butanol	55.99	7.23	16.80
2-Butanol	35.15	9.13	10.55
2-Methyl-1-propanol	17.36	10.79	5.21
2-Methyl-2-propanol	9.41	1.47	2.82
Methyl acetate	5.93	1.17	1.78
Ethyl acetate	4.83	.21	1.45
n-Butylamine	4.12	-	1.24
tert-Butylamine	4.22	-	1.27
n-Amylamine	5.65	-	1.70
iso-Amylamine	5.12	-	1.54
n-Hexylamine	14.90	-	4.47
Benzylamine	3.83	-	1.15
Propanoic Acid	8.73	1.93	2.62
Butanoic Acid	13.34	4.46	4.00
Pentanoic Acid	16.71	1.52	5.01
D_2O	6.32	1.42	1.90
Glycerol	5.80	.03	1.74

Table 7: Retention Data for CPS

Solutes	Average Retention time (minutes)	95% C.I.	Average Retention Volume (cm^3)
LiCl	4.21	.71	3.91
NaCl	4.61	.59	4.31
KCl	4.58	.24	4.28
RbCl	4.47	.43	4.17
NaF	4.74	.49	4.44
NaBr	4.53	.25	4.23
NaI	4.58	.06	4.28
KBr	4.26	1.39	3.96
CsBr	4.58	.04	4.28
$MgCl_2$	4.53	.08	4.23
$CaCl_2$	4.07	2.29	3.77
$SrCl_2$	4.52	.17	4.22
$BaCl_2$	4.20	.72	3.90
NH_4Cl	4.53	.10	4.23
Kbiphthalate	4.31	.73	4.01
Sucrose	4.22	1.11	3.92
Maltose	4.50	.14	4.20
Fructose	4.53	.17	4.23
D-Sorbitol	4.10	.95	3.80
Xylitol	4.18	.75	3.88
Raffinose	4.38	.19	4.08
Erthylitol	4.27	1.08	3.97
D-Glucose	4.44	.10	4.14
PAA 6000	4.50	.68	4.20
Ethylene glycol	4.71	.50	4.41
PEG 200	4.13	1.08	3.83
PEG 300	5.48	3.48	5.18
PEG 400	4.43	1.38	4.13
PEG 600	5.02	2.35	4.72
PEG 1000	4.44	.66	4.14
PEG 1530	3.51	3.17	3.21
PEG 2000	12.55	5.39	12.25
Methanol	4.77	.05	4.47
Ethanol	5.21	.29	4.91
1-Propanol	6.08	.85	5.78
2-Propanol	5.03	.02	4.73
1-Butanol	17.06	2.71	16.76
2-Butanol	4.48	.54	4.18
2-Methyl-1-propanol	5.13	.46	4.83
2-Methyl-2-propanol	4.55	.44	4.25
2-Pentanol	5.11	.68	4.81
3-Pentanol	4.67	.34	4.37
2-Methyl-1-butanol	4.93	.05	4.63
3-Methyl-1-butanol	4.54	.47	4.24
2-Methyl-2-butanol	4.70	.13	4.40
Methyl acetate	4.28	.70	3.98
Ethyl acetate	4.56	.52	4.26
n-Butylamine	9.87	.21	9.57
iso-Butylamine	5.35	.58	5.05
sec-Butylamine	5.26	.19	4.96
tert-Butylamine	5.27	1.79	4.97
n-Amylamine	7.37	6.46	7.07
iso-Amylamine	5.19	.43	4.89
n-Hexamylamine	7.26	2.94	6.96
Cyclohexylamine	5.28	.13	4.98
Benzylamine	10.25	9.61	9.95
Propanoic Acid	4.27	.68	3.97
Butanoic Acid	4.92	.42	4.62
Pentanoic Acid	5.18	.40	4.85
Ether	4.97	.97	4.67
MEEK	4.23	.57	3.93
D_2O	4.61	.02	4.31
Glycerol	4.48	.13	4.18

Table 8: Retention Data for TMS

5.3 Solute Distribution Coefficient (K'_a)

The solute distribution coefficient (K'_a) was described in section 3.3. In order to generate the coefficient for any one solute an appropriate minimum retention volume Vr_{min} must be defined.

The Vr_{min} is the sum of the system dead volume (V_d) and the volume of the mobile phase (V_m). V_d is the total amount of void spaces that exist in any LC system. The system dead volume includes the empty spaces in the detector and in the various connectors and fittings. This volume can be determined with ease and accuracy. The volume of the mobile phase is obtained with more difficulty. V_m is determined from the retention time of a theoretical solute that exists only in the mobile phase and is not affected by the stationary phase. Such a solute will travel the same path through the LC packing as a solvent molecule that only exists in the mobile phase and therefore provides an estimate of the volume of the mobile phase. Since such a solute is not affected by the stationary phase, the retention time should be the shortest and consequently the retention volume, the smallest. Two methods of estimating Vr_{min} for the polymer column were considered. The first method consisted of taking the minimum Vr of all solutes tested on a particular polymer column. After physicochemical considerations, a second method consisting of using the minimum Vr for a series of inorganic solutes were adopted. The Vr_{min} and the corresponding solute for each polymer are given in table 9.

Vr_{min} is also required to calculate the stationary volume (V_s). V_s is the difference between the retention volume of deuterium ($V_{r_{D_2O}}$) and the minimum retention volume (equation 30). V_s was calculated and compared using the two definitions for Vr_{min} (table 10).

PEG 1530 has the smallest retention volume of all the solutes for the TMS polymer (table 8). Similarly, PAA 6000 is the solute with the smallest retention volume for the other four polymers (table 4,6,5,and 7). The problem with this definition of Vr_{min} became apparent when the size of the molecule was taken into consideration. The Stokes radii for PEG 1530 and PAA 6000 is 9.95 A and 25.00 A [30]. The molecular size for these solutes is larger than the Stokes radius for

water (0.85 A). Therefore, steric effects could be contributing to the retention of those solutes. PAA 6000, being an acid, possesses a charged functional group. This violated the initial assumption of no interactions with the polymer. This violation combined with the steric effect were the reasons for rejecting the first method based on the overall minimum retention volume as the criteria for defining the minimum retention volume. This definition underestimates the minimum retention volume which resulted in an over prediction of the stationary phase volume (table 10).

Polymer	Method 1 Solute	Vr_{min} (cm^3)	Method 2 Solute	Vr_{min} (cm^3)
Udel	PAA6000	1.60	LiCl	1.93
Victrex	PAA6000	1.89	$MgCl_2$	2.01
Radel	PAA6000	2.18	$MgCl_2$	2.23
CPS	PAA6000	1.20	$BaCl_2$	1.58
TMS	PEG1530	3.21	$CaCl_2$	3.77

Table 9: Comparison of Minimum Retention Volume Generated from Two Different Methods

The second method of defining Vr_{min} produced a more reasonable estimate of V_s. Salts which had the lowest retention time varied from a monovalent salt such as LiCl (Udel) to a divalent salt for other polysulfones. Each salt had a Stokes radii ($<$ 1.96 A [13]) that was closer to the size of the mobile phase, therefore sterics would not contribute to the retention of these salts. Using the minimum retention time of a series of inorganics salts, the volume of the stationary phase for Udel (1.33 $\times 7$ m^3/g) matched the literature value for Udel (1.40 $\times 7$ m^3/g)[13]. This method was adopted as the definition for Vr_{min}.

The distribution coefficients for the various polymer systems were calculated using equation 32 and summarized in table 11 . The general trend of the liquid chromatography distribution coefficient for Victrex corresponded with the results

Polymer	V_s	
	Method 1 Overall Min.	Method 2 Salt Min.
	$(m^3/g \times 10^7)$	$(m^3/g \times 10^7)$
Udel	6.62	1.33
Victrex	6.49	3.49
Radel	2.24	1.42
CPS	9.58	4.12
TMS	1.12	5.40
Udel [31]	-	1.40

Table 10: Comparison of Calculated Stationary Phase Volume Based on the Two Definitions of Minimum Retention Volume

generated by Matsuura *et al.* [13]. Solutes such as sugars and inorganic salts had a distribution coefficient less than 1 for all polysulfones tested. The distribution coefficient for alcohols increased with the increase in carbon number. This increase in K_a' corresponded to the increase in the attraction of the polymer for the solute.

5.4 Interfacial Layer Thickness and Surface Excess

Table 12 lists the interfacial surface area of the chromatography column generated using the method described in section 3.4. There was a difference in specific surface area due to the particle production methods. Packing produced from direct crushing had a specific surface area of 0.26 m^2/kg of polymer (Radel) to 0.47 m^2/kg of polymer (Victrex). The area for the same material produced by the spraying method ranged from 16.92 m^2/kg of polymer (Radel) to 20.67 m^2/kg of polymer (Victrex). The specific surface area for particles made from spraying was two orders of magnitude greater than the particles made from direct crushing. This large specific

Solute	Udel	Victrex	Radel	CPS	TMS
LiCl	0	1.13	1.18	.11	.26
NaCl	.35	1.29	.84	.13	1.01
KCl	.25	.80	1.00	.22	.95
RbCl	.69	1.14	.98	.13	.74
NaF	.35	1.22	2.28	1.95	1.23
NaCl	.35	1.29	.84	.10	1.01
NaBr	1.18	.83	1.77	.46	.86
NaI	.41	1.57	.66	.18	.94
KBr	.31	.61	.52	.05	.36
CsBr	.35	.70	1.78	.61	.95
$MgCl_2$	.21	0	0	.13	.86
$CaCl_2$	.39	.57	1.30	.12	0
$BaCl_2$	1.42	.67	.77	0	.83
$SrCl_2$	.71	1.21	1.92	.01	.26
NH_4Cl	.01	2.62	.72	.36	.85
Kbiphthalate	.19	.70	6.62	.09	.44
Ethylene Glycol	.83	1.10	1.50	.50	1.19
PEG 200	3.25	2.18	4.99	2.50	.11
PEG 300	9.71	3.57	13.84	4.05	2.61
PEG 400	34.16	8.48	73.39	8.27	.67
PEG 600	-	31.59	1.57	21.78	1.75
PEG 1000	-	1.48	-	.03	.69
PEG 1530	-	.98	-	-	-
PEG 2000	-	-	-	-	15.64
Sucrose	0	.99	1.48	.36	.28
Maltose	.35	1.30	1.27	.43	.80
Fructose	2.03	1.26	1.39	.50	.86
D-Sorbitol	.09	1.49	.96	.63	.06
Xylitol	.88	1.18	1.21	.85	.22
Raffinose	1.94	1.53	2.17	.36	.57
Erthylitol	.08	2.43	1.53	.49	.37
D-Glucose	.09	1.46	.86	.36	.69
Methanol	1.64	2.02	3.27	1.15	1.31
Ethanol	7.79	3.82	8.96	3.39	2.11
1-Propanol	26.88	13.92	36.94	11.75	3.71
2-Propanol	16.84	7.83	20.63	8.68	1.77
1-Butanol	-	57.81	75.10	47.32	23.95
2-Butanol	75.82	26.92	117.75	27.89	.76
2-Methy-1-propanol	35.49	26.08	-	11.29	1.96
2-Methy-2-propanol	3.15	1.67	4.62	3.88	.89
1-Pentanol	8.35	39.47	-	-	-
2-Pentanol	-	79.88	-	-	1.92
3-Pentanol	-	-	-	-	1.12
2-Methyl-1-butanol	-	-	-	-	1.59
3-Methyl-1-butanol	-	.96	-	-	.88
2-Methyl-2-butanol	-	4.06	-	-	1.16
Methyl acetate	.85	.77	9.81	.63	.33
Ethyl acetate	-	2.07	7.33	-	.91
N-Butylamine	.14	22.26	131.58	-	10.69
Iso butylamine	-	11.89	-	-	-
Sec butylamine	-	20.22	-	-	-
Tert Butylamine	1.07	5.77	65.18	-	2.37
N-Amylamine	-	105.01	40.84	.37	2.20
Iso Amylamine	-	41.07	-	-	2.22
N-Hexylamine	-	135.66	-	9.00	6.08
Benzylamine	-	-	-	-	2.07
Propanoic Acid	32.21	21.81	38.50	3.24	.37
Butanoic Acid	3.90	-	179.78	7.54	1.58
Pentanoic Acid	-	-	-	10.69	1.99
Glycerol	.29	2.07	1.07	.52	.76

Table 11: Partition Coefficient for Various Polysulfones

surface area indicated the presence of internal spaces accessible to water in particles made by spraying. The inability of the mechanical crushing particle production method to introduce such internal voids in the 38-53 μm particles resulted in the low specific surface area for the chromatography column. Less contact area means less surface interactions between solute and polymer. This factor contributed to the low retention resolution between different solutes for the crushed particle columns. The initial LC data comparisons (table 3) did not show any difference in retention times between solutes for columns packed with crushed particles.

Polymer	Specific Surface Area m^2/kg of polymer	T_i Angstrom (A)
Crushed Udel	.39	-
Crushed Victrex	.47	-
Crushed Radel	.26	-
Sprayed Udel	18.56	7.17
Sprayed Victrex	20.67	16.84
Sprayed Radel	16.92	8.39
Sprayed CPS	6.38	64.58
Victrex [13]	14.47	8.3

Table 12: Packing Specific Surface Area and Interfacial Water Layer Thickness for Various Polysulfones

The volume of the stationary phase (section 5.3) was divided by the specific surface area to obtain an estimate of the interfacial water thickness (T_i) [13]. The values for T_i were in the order of molecular dimensions. This is expected since the influence of these surface forces appears on a molecular level. The interfacial area was used to generate surface excess values (Γ) for the solutes listed in table 13. A negative surface excess indicates rejection for a particular solute. A large positive surface excess indicates preferential sorption of the solute.

Solute	Udel	Victrex	Radel	CPS
LiCL	-71.70	22.53	15.39	-573.96
NaCl	-46.66	48.82	-13.47	-561.79
KCl	-53.78	-34.18	-.00	-502.09
RbCl	-22.47	23.20	-1.92	-562.60
NaF	-46.66	37.92	107.76	612.52
NaCl	-46.66	48.82	-13.47	-581.07
NaBr	12.80	-28.81	64.27	-348.09
NaI	-42.36	95.77	-28.87	-528.85
KBR	-49.79	-65.73	-40.40	-614.87
CsBr	-46.66	-50.70	65.43	-251.98
$MgCl_2$	-56.62	-169.00	-83.90	-559.72
$CaCl_2$	-43.81	-73.23	25.02	-568.88
$BaCl_2$	30.16	-56.33	-19.24	-646.00
$SrCl_2$	-21.05	35.68	76.98	-638.89
NH_4Cl	-70.84	273.77	-23.10	-415.33
Kbipthalate	-58.04	-50.71	471.48	-585.75
PAA 6000	-355.37	-311.71	-132.78	-1399.08
Ethylene glycol	-12.23	16.89	42.34	-321.00
PEG 200	161.04	199.04	334.84	971.06
PEG 300	624.82	434.89	1077.67	1969.83
PEG 400	2377.74	1263.74	6073.86	4694.05
PEG 600	-	5169.52	48.10	13421.99
PEG 1000	-	81.09	-	-625.92
PEG 1530	-	-3.35	-	-
PEG 2000	-	-	-	-
Sucrose	-75.11	-1.88	40.41	-412.90
Maltose	-46.69	50.70	23.05	-366.19
Fructose	74.18	43.19	32.71	-324.74
D-Sorbitol	-65.15	82.62	-3.46	-240.99
Xylitol	-8.25	30.75	17.32	-97.06
Raffinose	67.15	90.13	98.14	-415.11
Erthylitol	-66.30	242.22	44.27	-328.03
D-Glucose	-65.15	76.99	-11.93	-415.06
Methanol	45.53	172.75	190.52	97.06
Ethanol	486.83	476.95	667.77	1546.35
1-Propanol	1855.38	2183.85	3015.55	6945.26
2-Propanol	1135.56	1154.83	1647.29	4963.76
1-Butanol	-	9601.08	6217.03	29922.87
2-Butanol	5364.47	4380.89	9795.25	17368.84
2-Methyl-1-Propanol	2472.80	4238.10	-	6647.35
2-Methyl-2-Propanol	154.21	112.66	304.06	1860.98
1-Pentanol	526.65	6500.71	-	-
2-Pentanol	-	13330.19	-	-
3-Pentanol	-	-	-	-
2-Methyl-1-Butanol	-	-	-	-
3-Methyl-1-Butanol	-	-7.52	-	-
2-Methyl-2-Butanol	-	516.37	-	-
Methyl Acetate	-11.10	-39.48	738.97	-237.66
Ethyl acetate	-	180.27	531.14	-
N-Butylamine	-61.32	3592.17	10955.66	-
Iso-Butylamine	-	1840.22	-	-
Sec-Butylamine	-	3248.56	-	-
Tert Butylamine	5.26	806.50	5384.50	-
N-Amylamine	-	17576.94	3342.70	-405.01
Iso-Amylamine	-	6772.20	-	-
N-Hexamylamine	-	22756.77	-	5167.94
Benzlamine	-	-	-	-
Propanoic Acid	2238.06	3516.70	3146.42	1449.29
Butanoic Acid	207.98	-	15000.00	4227.40
Pentanoic Acid	-	-	-	6259.11
Glycerol	-51.21	180.27	5.78	-312.69

Table 13: Surface Excess for Various Polysulfones

Chapter 6

Discussion

The discussion focuses on three aspects of the liquid chromatography data summarized in chapter 5. The first aspect concerns the variation in retention time with different solutes corresponding to a particular polymer and water system. The second part of the discussion deals with the differences between the five polymers tested and their effects on the retention characteristics of a solute. Finally, the chromatographic results are discussed in relation to membrane performance. LC data should ultimately be used as a tool for predicting solute separation and solute flux.

6.1 Physicochemical Property of a Molecule and its Relation to LC Data

Chromatography can be used to evaluate the interactions between the solute and polymer in an aqueous environment. This method can produce distribution coefficients for solutes for the same polymer-solvent systems. Difference in coefficients is then due to the differences in physical and/or chemical properties of each solute. Parameters that can quantify solute property differences can also describe the change in K'_a. Such parameters can therefore be used to predict the behavior of the solute at the polymer interface.

The strength of the mutual affinity between solute and water is one of the physical characteristics for the solute. The lipophilic (or hydrophobic) nature of any solute (i) can be described by a liquid-liquid partition coefficient (P_i). The coefficient quantifies the distribution of a substance between an immiscible organic phase and an accompanying aqueous phase. A large value P_i indicates a more hydrophobic nature and a small value means a more hydrophilic nature.

A partition coefficient is system specific. This means that the value can only be applied to a specific organic phase. However, partition coefficients generated from different organic solvent-water systems can be related using the general Collander equation [32] :

$$\ln P_a = m \ln P_b + b \tag{49}$$

where

P_a, P_b – Partition coefficients involving different organic solvents a and b respectively

m, b – Proportionality constants (slope,intercept respectively)

Generally, the octanol-water system was chosen as the frame of reference for comparing solute partition behavior in different solvent systems. The reason being that partitioning data for a great number of biologically interesting solutes have already been generated for this system.

This type of relationship has been extended to include the data generated by liquid-liquid chromatography [33] systems involving two immiscible phases (i.e. a water phase and an organic phase). The capacity factor (k'_a-defined in section 3.2) generated in a liquid chromatography system is considered to be analogous to a liquid-liquid partition coefficient. Thus, k'_a can be related to the octanol-water ($P_{o/w}$) in a fashion similar to the Collander equation :

$$\ln k'_a = m \ln P_{o/w} + b \tag{50}$$

The relationship is general enough to cover cases involving classical adsorption experiments [34], as well as liquid-solid chromatography [35,36].

There is a linear relationship between the logarithm of the partition coefficients in a model system (ie. octanol-water) and the logarithm of partition coefficients from any other organic solvent-aqueous phases. An extension of the Collander equation is applied to this work. The equilibrium coefficient (K_a') between a surface influenced stationary phase and the mobile phase is related to the octanol-water partition coefficient.

The octanol-water partition coefficient ($P_{o/w}$) for many solutes has been reported by Hansch and Leo [37]. The values for a series of alcohols, amines and propanoic acid are tabulated in table-14. The natural logarithm of the octanol-water coefficient was plotted against the natural logarithm of the equilibrium constant generated by liquid chromatography for the five polymers under study (figures 14-18). A linear relationship was obtained for four of the polysulfones tested (Udel, Radel, Victrex, CPS) but not for TMS. A linear regression was also performed on the data to quantify that a high degree of correlation existed between experimental values and the octanol-water partition coefficient obtained from the literature. The parameters (slope,intercept) generated by the regression and the correlation coefficient (R) are summarized in table 15.

The correlation coefficient between $\ln K_a'$ and the natural logarithm of the octanol-water partition coefficient for four polymers was better than 96 percent. The equation

$$\ln K_a' = m \ln P_{o/w} + b \tag{51}$$

could be used to relate the partitioning behavior of a solute in an octanol-water system to the distribution of a solute between water and the polymer influenced water layer. The validity of equation 51 substantiates the basic assumption that the calculated K_a' does indeed measure a polymer induced partitioning effect. By drawing a parallel between the octanol-water system and the liquid chromatography system, the stationary phase could be interpreted as possessing properties similar to the non-aqueous component of the octanol-water partition coefficient.

In the case of trimethylsilyl polysulfone (TMS) there was no correlation between the natural logarithm of K_a' and the natural logarithm of $P_{o/w}$. This indicated that the column did not generate partition data. The reason being that the addition

Solute	ln ($P_{o/w}$)	$^1\chi$
Methanol	-.70	1
Ethanol	-.31	1.41
1-Propanol	.28	1.91
2-Propanol	.05	1.73
1-Butanol	.88	2.41
2-Butanol	.75	2.27
2-Methy-1-propanol	.61	2.27
N-Butylamine	.87	-
Tert Butylamine	.40	-
Propanoic Acid	.29	-

Table 14: Octanol-Water Partition Coefficients and First Order Connectivity Indices for Selected Solutes [37]

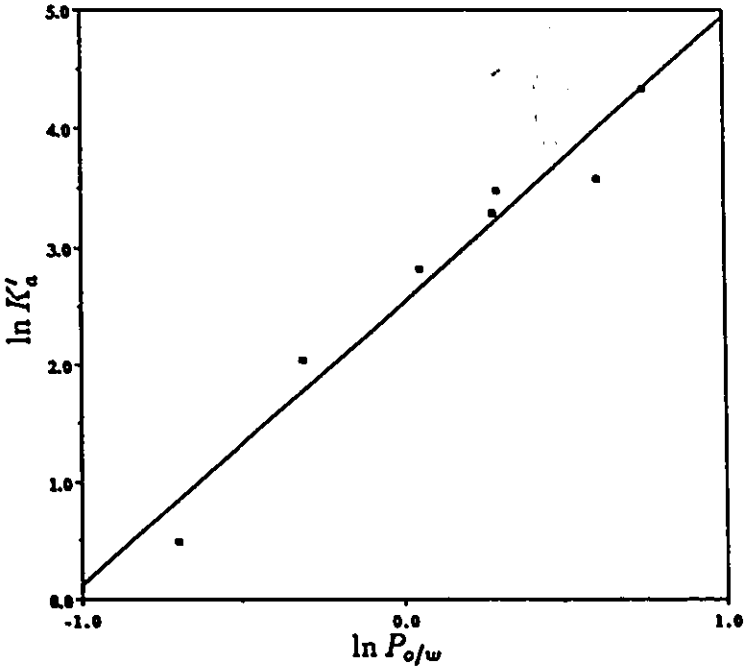

Figure 14: Relation between LC Partition Coefficient and Octanol-Water Partition Coefficient for Udel

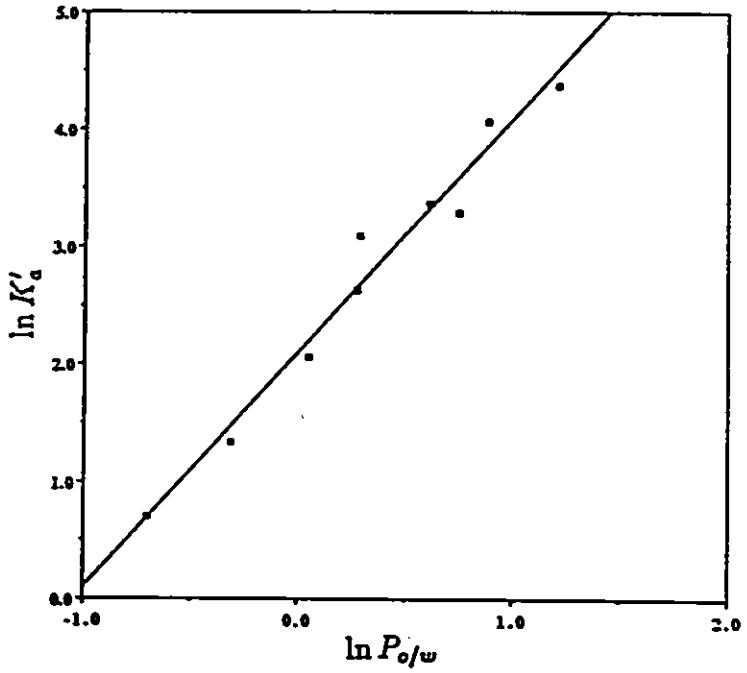

Figure 15: Relation between LC Partition Coefficient and Octanol-Water Partition Coefficient for Victrex

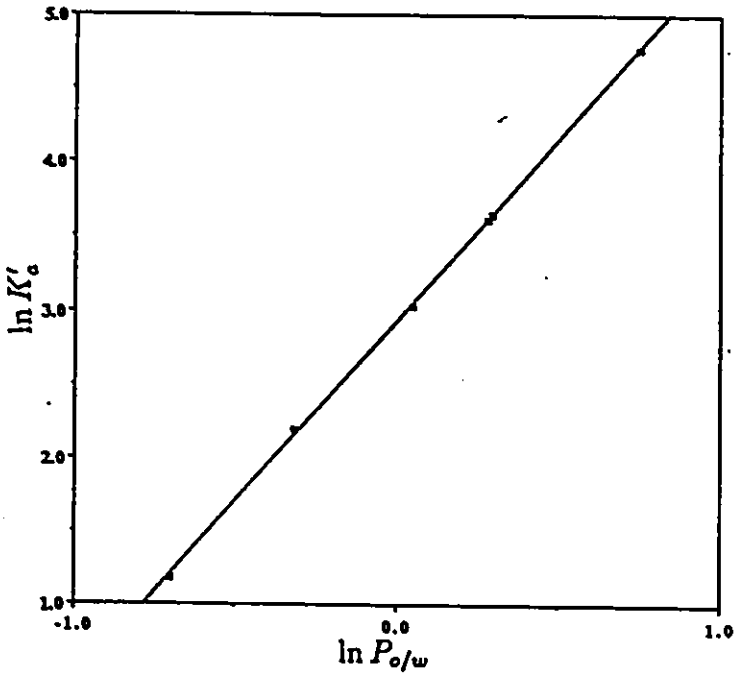

Figure 16: Relation between LC Partition Coefficient and Octanol-Water Partition Coefficient for Radel

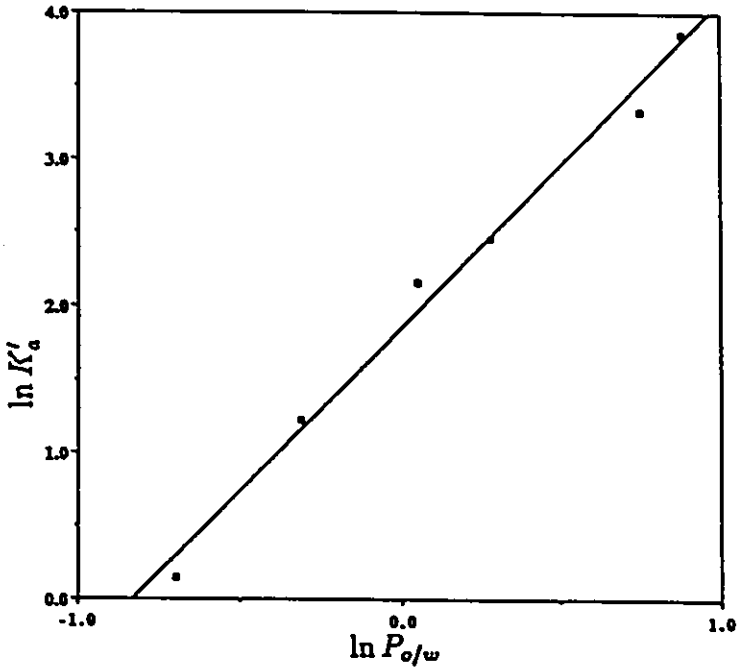

Figure 17: Relation between LC Partition Coefficient and Octanol-Water Partition Coefficient for CPS

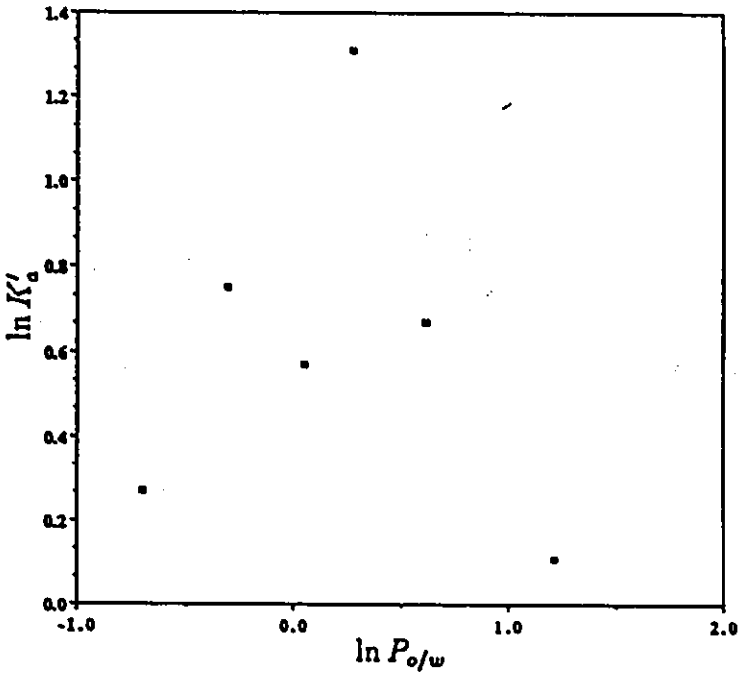

Figure 18: Relation between LC Partition Coefficient and Octanol-Water Partition Coefficient for TMS

Polymer	Regression Coefficient	Slope	Intercept
Udel	.9[illegible]	2.411	2.526
Radel	.9[illegible]	2.231	2.912
Victrex	.920	1.820	1.892
CPS	.968	2.079	1.763
TMS	.085	-	-

Table 15: Linear Regression for ln K'_a vs. $P_{o/w}$

of a tri-methylsilyl group increased the hydrophobicity of the polysulfone to such an extent that the stationary phase was small or negligible. Therefore, the solute was only under the influence of the mobile (water) phase. The retention data for the TMS polymer did not reflect the surface influence of the polymer and the K'_a generated for this polymer cannot be accepted.

The slope generated by equation 51 describes the deviation in behavior of the stationary phase in the LC system in comparison to the octanol phase in the octanol-water system. A slope of greater than one means that the stationary phase behaves in a more lipophilic manner when compared to the octanol phase; conversely, a slope of less than one means that the stationary phase behaves in a more hydrophilic manner than the octanol phase. The difference in slopes between the four tested polymers was small. The slopes ranged from 1.82 for Victrex to 2.40 for Udel. The slopes showed that the equilibrium distribution generated by LC deviated in behavior from an octanol-water system (ie. the interfacial layer was more lipophilic than octanol). The values of the slopes cannot compare lipophilicity between one polymer and another because the difference between slopes is small.

The octanol-water partition coefficient for numerous substances has been tabulated by Hansch and Leo [37]. It is conceivable that $P_{o/w}$ values could be used as a rough guideline for predicting the surface (retention) properties of a solute on a particular polymer. Once surface interactions are estimated then further manipulation

of the material to form a membrane can be considered.

The distribution of the solute between two phases is partially affected by the physical structure of the solute molecule. Structural information can be encoded and converted into numerical values (indices) . The molecular connectivity index (χ) is one type of topological index and has already been used to predict retention behavior for liquid-liquid chromatography systems [38,39].

The molecular connectivity index is a general systematic method of categorizing any large molecule according to its atomic structure. The formalism 'molecular connectivity' is denoted by the Greek letter 'chi' and is adopted by Kier and Hall [40]. In their definition, the structural formula is written down as a molecular skeleton in which all atoms (except hydrogen) are identical. Each carbon atom is designated by a cardinal number (δ_i). This number (δ_i) is a count of the adjacent (formally bonded) carbons for the ith carbon. $^1\chi$ is then defined by summing the reciprocal root of all possible combinations of adjacent cardinal numbers. That is:

$$^1\chi = \sum(\delta i \times \delta j)^{-0.5} \tag{52}$$

The prefix 1 represents a one-bond dissection of the molecule. Higher order indices ($^2\chi$,$^3\chi$) involving two or greater adjacent atoms can also be defined. An increase in $^1\chi$ means an increase in the degree of branching and/or an increase in the chain length.

Polymer	Regression Coefficient	Slope	Intercept
Udel	.978	2.487	-1.690
Radel	.988	2.319	-1.800
Victrex	.980	2.488	-1.267
CPS	.956	2.311	-2.065
TMS	.140	-	-

Table 16: Linear Regression for ln K'_a vs. $^1\chi$

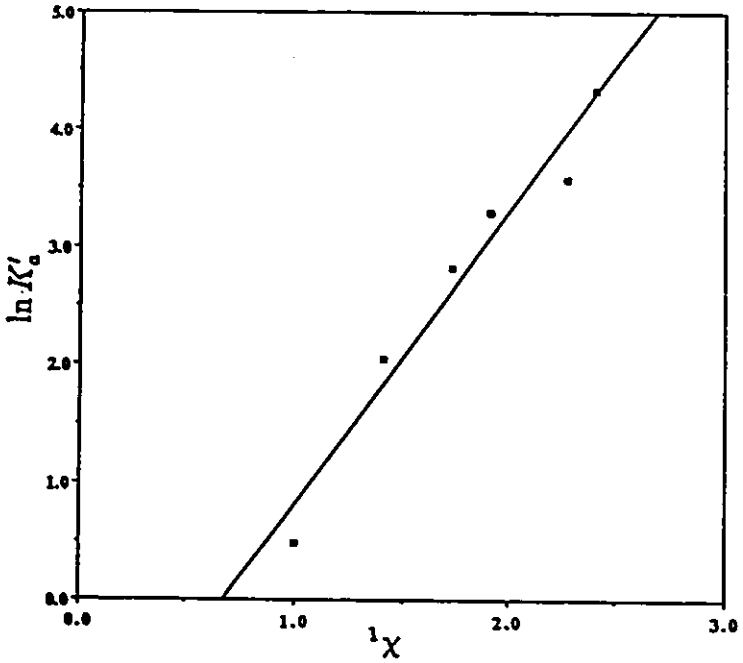

Figure 19: Relation between LC Partition Coefficient and First-Order Connectivity Index for Udel

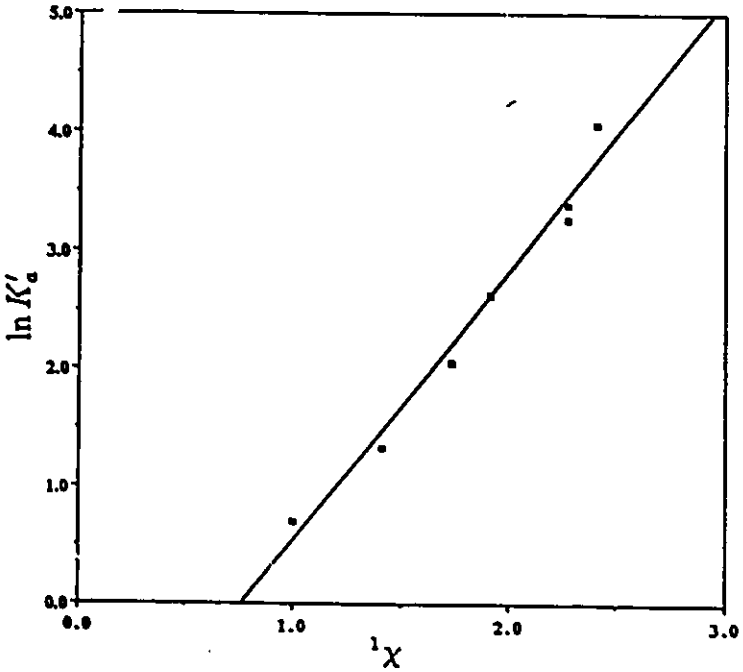

Figure 20: Relation between LC Partition Coefficient and First-Order Connectivity Index for Victrex

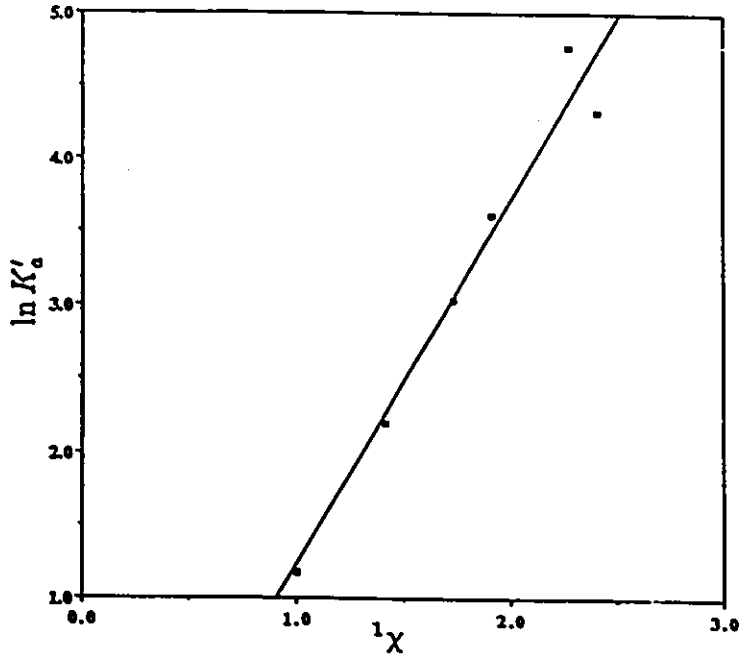

Figure 21: Relation between LC Partition Coefficient and First-Order Connectivity Index for Radel

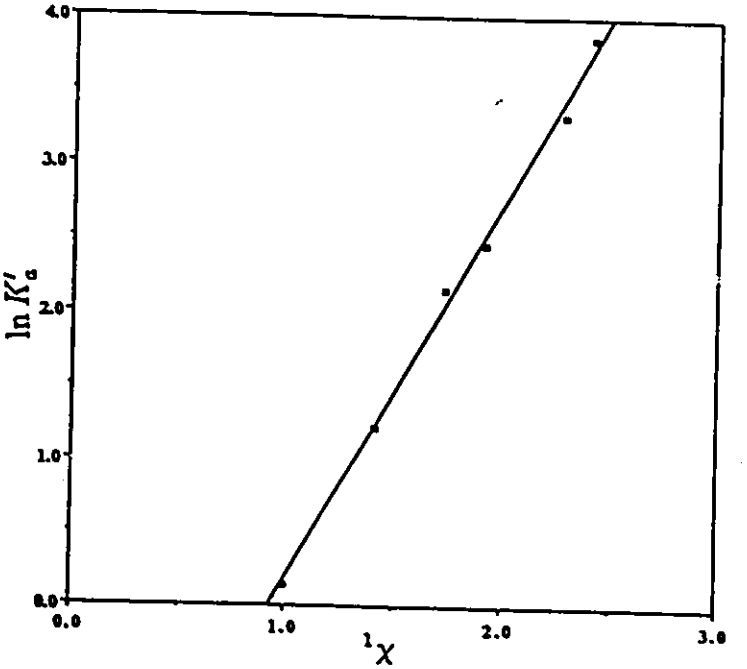

Figure 22: Relation between LC Partition Coefficient and First-Order Connectivity Index for CPS

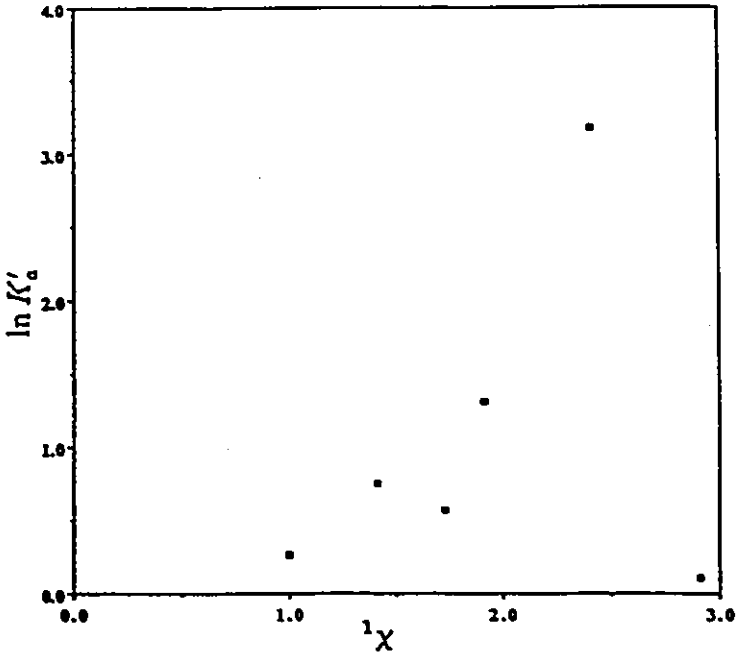

Figure 23: Relation between LC Partition Coefficient and First-Order Connectivity Index for TMS

The natural logarithm of the equilibrium distribution coefficient of alcohols with less than four carbon atoms was plotted against the corresponding $^1\chi$ value (figure 19-figure 23). The plots show linear behavior for four polymers (Udel, Victrex Radel and CPS) and scatter for the remaining polymer (TMS). The correlation coefficient, the slope and the intercept for each of the polymer system is summarized in table 16. Correlation coefficients for four of the polysulfones were greater than 95%. A direct linear relationship between $^1\chi$ and K'_a was confirmed both by the plots and the correlation coefficient. An increase in the number of carbon atoms or branching of an alcohol led to an increase in $^1\chi$ and this corresponded to an increase in the natural logarithm of K'_a. In general, the higher the number of carbon atoms in an alcohol structure the larger the affinity of the solute for the polymer and consequently the longer the retention time in a LC system. Similarly, there is a corresponding increase of K'_a with n increase in branching of the alcohol. There are practical limits to this relationship. It is no longer valid when the alcohol is not completely miscible in water or when the affinity between the polymer and solute is so strong that the solute no longer is eluted from the chromatography column.

The TMS column results did not correlate with the topological descriptor. The

logarithmic plot of ln K'_a vs. $^1\chi$ showed that the data is scattered. This lack of correlation is attributed to the increase in hydrophilicity due to the addition of a silyl group to the Udel polysulfone. There is insufficient active surface area in the TMS column for the water to generate a stationary phase so that a partitioning effect could be observed.

A topological index that was derived from information contained solely in the structural formula can be related to the behavior of the solute at a polymer interface (K'_a). The advantage of such a relationship can clearly be seen. Once the equilibrium coefficient for one solute and one polymer is obtained then the K'_a for other solutes in the same series can at least be approximated. The disadvantage of using $^1\chi$ is that only the physical structure is described. The index does not take into account the change in the functional group of the solute. Therefore, the relationship holds only for a homologous series with the same active groups.

Actions of different solutes on the polymer-solution interface result in a change in the partition value generated by liquid chromatography. The nature of this interaction is a partitioning effect that is a function of the chemical and physical property of the solute molecule. Quantitative description of the solutes can be related to the equilibrium coefficient for a specific polymer. Such descriptions can be used as predictive tools for surface interactions.

6.2 Polymer Solubility Parameters and LC Retention Data

Total solubility parameter (δ_t) is the square root of the cohesive energy density [41]. Cohesive energy density is defined as the cohesive energy per unit volume of the molecule. Cohesive energy is associated with the net attractive interactions between individual molecules. Solubility parameters can be used to describe the cohesive and adhesive properties of the polymer. This study stresses the existence of a link between this physical property (ie. strength of attraction between molecular units of a polymer) and solute interactions at the polymer solution interface.

A relationship between δ_t and partitioning or surface effects has already been suggested for different systems. In liquid-liquid chromatography systems, the polarity of the mobile phase and the stationary phase is characterized by their solubility parameter[42]. The retention of a solute in different mobile and stationary phases is related to the change in δ_t. For membrane systems [43], difference in membrane performance (ie. flux and separation) for different membrane material is related to the difference in the material's solubility parameter. For this study, the difference in total solubility parameter for the polysulfones studied was calculated and compared to the equilibrium constants generated by liquid chromatography. The difference in the physicochemical properties of the polysulfone are explained in terms of the difference in their solubility parameter.

The total solubility parameter (δ_t) can best be described by its applications and its components. The most common use of δ_t for polymers is to estimate the compatibility between a solvent and the polymer. A polymer is likely to be dissolved in a solvent if the solubility parameter of the two are the same. Hansen [44] used a quantity known as the total solubility parameter as a measure of the forces that exist on a molecular level. The total solubility parameter can be broken down into three components. δ_d corresponds to the contribution of the dispersion forces. δ_p describes the contribution of polar forces. δ_h is the contribution of the hydrogen bonding force. Dispersive forces are intermolecular forces of attraction caused by fluctuating dipoles. Polar forces are due to a net separation of charge caused by non-symmetric molecules which contain atoms of different electronegativities. The electron cloud of a hydrogen atom can be pulled away from the nucleus by a strongly negative atom to which the hydrogen is covalently attached. Hydrogen bonding occurs when the exposed nucleus is allowed to interact with a neighboring structure which contains a lone pair of electrons. The three types of forces together characterize the attractive forces at a molecular level. The increase in δ_h and δ_p and consequently the increase in δ_t means a more hydrophilic polymer. Conversely, as δ_t decreases the polymer is considered more lipophilic. δ_d and δ_p are grouped together and are described by a single solubility parameter (δ_v).

For this study, the actual solubility parameters were not available for many

polymers. Experiments to evaluate the actual solubility parameters were considered to be too time consuming. The solubility parameters were therefore estimated from group contributions. Table 17 summarizes the solubility parameters for the family

	Udel	Radel	Victrex	CPS	TMS
Experimental $((\delta_t)_e)$	22.1 [13]	-	22.6 [45]	-	-
Fedors $((\delta_t)_f)$ [46]	25.28	26.59	28.37	25.58	21.5
$(\delta_t)_{hv}$ [46]	19.92	18.13	21.24	20.41	-
δ_v [46]	18.67	16.99	18.86	18.30	-
δ_h [46]	7.29	6.28	9.77	7.78	-

Table 17: Solubility Parameters ($J^{\frac{1}{2}}cm^{\frac{3}{2}}$) for Various Polysulfones

of polysulfones. The table contains two different methods of calculating δ_t as well as estimates for the component solubility parameters (δ_v,δ_h). The first method calculates $(\delta_t)_f$ based on structural group contributions to the cohesive energy and the molecular volume tabulated by Fedors [47]. The advantage of this method is that Fedors reported values for a large number of functional groups. The second method estimated the component solubility parameter from the structure of the repeating unit [13]. $(\delta_t)_{hv}$ was obtained as the square root of the sum of the squared component solubility parameters (ie. $(\delta_t)_{hv} = \sqrt{\delta_h^2 + \delta_v^2}$).

Calculated solubility parameters are compared to available experimental values for two commercial polysulfones in table 17. The experimental total solubility parameter $((\delta_t)_e)$ for Udel and Victrex is 22.1 $J^{\frac{1}{2}}cm^{\frac{3}{2}}$ and 22.6 $J^{\frac{1}{2}}cm^{\frac{3}{2}}$ respectively. Calculated total solubility parameter $((\delta_t)_f)$ based on the results of Fedors are 25.28 and 28.37 respectively. According to component solubility parameter $((\delta_t)_{hv})$ the values are 19.92 and 21.24. Fedor's method overestimated the solubility of a polymer by 2 $J^{\frac{1}{2}}cm^{\frac{3}{2}}$ while the component solubility parameters underestimated the value by 1 $J^{\frac{1}{2}}cm^{\frac{3}{2}}$. Calculated solubility parameters $((\delta_t)_f$,$(\delta_t)_{hv})$ showed a larger difference between Victrex and Udel than the experimental values. This means that

calculated values are not accurate enough to predict the cohesive energies of polysulfones. Polymers with different repeating groups cannot be compared solely on values generated by group contributions because group contributions are insensitive to the particular arrangement of the molecules that produced the overall cohesive property of the polymer.

The difficulty of comparing δ_t of different repeating units can be avoided if the concept of structural contribution to solubility is applied to compare functional groups existing on the same repeat unit. The repeat unit can serve as a reference standard to which cohesion parameters can be compared. In this study, three polymers (Udel, CPS, TMS) had virtually identical repeating structures. They differed in the addition of a functional group (carboxyl, trimethyl silane) on the bisphenol portion of the Udel backbone.

The difference in behavior between CPS and Udel can be explained by the difference in component solubility parameter. Component solubility parameters in table 17 indicate that adding a carboxyl group to Udel increases δ_h by 0.5 $J^{\frac{1}{2}}cm^{\frac{3}{2}}$ and decreases δ_v by 0.37 $J^{\frac{1}{2}}cm^{\frac{3}{2}}$ δ_t increased by 0.5 $J^{\frac{1}{2}}cm^{\frac{3}{2}}$. δ_h shows CPS can form more hydrogen bonds. This results in an increase in the polymer's attraction for water. This increase in the hydrophilicity of the material is demonstrated by a thicker interfacial pure water layer (7 A for Udel vs. 65 A for CPS - see table 12) and greater rejection of inorganics and carbohydrates.

The group contribution method proposed by Fedors is more comprehensive in that there is an estimate for the silane functional group. $(\delta_t)_f$ generated for the TMS polymer was much lower than ordinary Udel polysulfone. This is a further indication of the hydrophobic nature of the polymer.

6.3 Relation to Membrane Performance

Liquid chromatography experiments can provide a guideline for determining the appropriate membrane material for a solute-solvent system. The addition of a carboxylated group onto a Udel backbone increases the total solubility parameter of the polymer. The physical property of the modified polymer is changed and

the CPS is described as being more hydrophilic than a Udel polysulfone. The consequence of this increase in hydrophilicity is a high rejection capability for salts and sugars and a greater attraction for water. This is shown by the retention times of those solutes in LC experiments and thicker calculated interfacial water layer. These two results are related to membrane performance. The critical pore size (r_c) needed to achieve a high separation of salts from water is much larger for the CPS than for the Udel polymer. Therefore, from the view point of the SFPF model, a membrane made from CPS can have both higher permeation and separation than conventional polysulfone membranes.

Membrane	Product rate $g/(hr \cdot cm^2)$	Separation %
CPS-A	51.48	16.09
CPS-B	15.54	45.07
Udel-A	2.71	10.07
Udel-B	7.58	9.79

Table 18: Comparison of CPS and Udel Membrane Performance for 2000 ppm NaCl [44]

Membrane	Product rate $g/(hr \cdot cm^2)$	Separation %
CPS1	.189	93.25
CPS2	.208	93.66
CPS3	.321	91.34
CPS4	.271	93.26

Table 19: Performance of Several CPS Membranes for 2000 ppm NaCl [44]

Membranes made from the two different material (CPS, Udel) were tested at 500

psi with a feed concentration of 2000 ppm NaCl (table 18). The results [48] showed that membranes cast from the same casting formulation and casting conditions produced sodium chloride separations that were vastly different. Udel polysulfone could only achieve a separation of 10%, while carboxylated polysulfones could achieve a 45% separation. The casting composition and casting conditions were changed so that up to 90% separation could be achieved (table 19). This rejection is high enough to compete with commercially available thin film composites. Therefore, this material should be examined further as the basis for a reverse osmosis desalination membrane.

Table 20 lists the separation characteristics for a series of polymers and sugars. The membranes made from this material show great promise in separating sugars because of the high separation and high flux. The results indicate that the carboxylated polysulfone can be developed as a nanofiltration membrane. This area of nanofiltration is especially important in the expanding field of Biotechnology where the desired separation falls between the range of Reverse Osmosis and Ultrafiltration [49,50].

Solute	CPS Membrane		
	PWP (g/hr)	PR (g/hr)	Separation %
Sucrose	188.80	153.1	59.38
Sorbital	232.27	198.3	48.77
PAA 6000	156.67	201.9	96.34
PEG 2000	200.13	143.6	77.82
PEG 3000	133.87	119.2	96.21
PEG 4000	149.07	109.2	95.78
PEG 6000	163.33	110.8	76.34
PEG 12000	154.67	110.0	79.28
PEG 15000	136.27	99.2	98.28

Table 20: Performance of a CPS Membrane for Various Solutes [44]

Chapter 7

Conclusion

A two fluid spray nozzle was designed to produce spherical chromatography packing in the 35-53 μm range. The spraying method was compared to other column packing production methods and was found to be superior due to higher bulk density, and larger internal surface area, as well as better retention time resolution between different solutes. Dry packing of particles in to chromatography columns proved to be adequate for the present study.

The equilibrium distribution coefficient (K_a') (between the bulk concentration and the interfacial concentration) and the surface excess (Γ) were generated for a series of inorganic and organic solutes. The behaviour of K_a' for all polysulfones studied is as follows :

$$\text{inorganics,carbohydrates} < 1 < \text{amines} < \text{alcohol,PEG's.}$$

The solute is rejected when K_a' is less than one and the solute is adsorbed K_a' is greater than one. This concept of preferential attraction or rejection can be illustrated more clearly by the calculated values of the surface excess. A negative value of the surface excess means a lower solute concentration in the interfacial layer than in the bulk solution. Similarly, a positive surface excess means a higher solute concentration near the polymer surface than in the bulk solution.

The interfacial water layer increases with the increase in water affinity of the polymer. Udel polysulfone modified by the addition of a carboxylate group has the

thickest interfacial layer (65 A). Commercially available polysulfones such as Udel, Radel, and Victrex have smaller interfacial layers (7.17 A, 8.39 A, and 16.84 A respectively).

Different solutes have different K'_a values. Each solute can be characterized by a physicochemical descriptor such as the octanol-water distribution coefficient ($P_{o/w}$) or by a topological descriptor such as the first order molecular connectivity index ($^1\chi$). A linear relationship was found between the logarithm of the experimentally generated LC partition coefficients and the logarithm of $P_{o/w}$. Similar linear behaviour was observed for $\ln K'_a$ and $^1\chi$. Solute retention behavior in liquid chromatography can be estimated from the properties of the solute.

Hansen solubility parameters were used to characterize the different polysulfones tested. Solubility parameters calculated from group contributions were not sensitive enough to quantify the change in the nature of the polymer due to the addition of a functional group to the back-bone. Component solubility parameter indicated that the addition of a carboxylate functional group increased the hydrogen bonding ability of the polymer and decreased the dispersion effects when compared to the unmodified polymer backbone (Udel). This result was used to explain the low K'_a values for CPS when compared to commercial polysulfone, and the high value for the pure water layer (T_i).

Carboxylated polysulfone (CPS) showed a strong rejection towards sugar and inorganic ions. The thickness of the interfacial water layer indicates that this type of modified polysulfones was also more hydrophilic than ordinary polysulfone. Preliminary membrane experiments support the conclusions made by the series of liquid chromatography experiments. Membranes made from CPS showed high NaCl rejection as well as high sugar separation.

Chapter 8

Recommendations

From this work, the following recommendations can be made. The experimental techniques can be improved as follows : a better spray nozzle can be developed and experimental scatter must be reduced. The concept of a distribution coefficient from liquid chromatography can be refined if a "true" void volume can be established. The calculated Hansen's solubility parameters should be verified experimentally. The analogy between membranes and chromatography can be extended to non-aqueous systems.

Spraying of the polymer solution proved to be an effective method of producing chromatography packing. However, chromatographic performance can be improved if the nozzle can be designed to produce even finer particles. In order to obtain smaller particles, the particle containment system must be even more efficient to minimize the lost valuable polymer.

A more accurate solvent delivery system is necessary in order to determine retention time differences between inorganic salts of different ionic sizes and carbohydrates of different molecular weights. The problem of reproducibility between different injections can also be over come by increasing the number of injections for each solute tested. This is only feasible if the injection of solutes can be automated.

The concept of V_m has to be more rigorously defined based on basic chromatography research. This will eliminate the seemingly arbitrary definition of Vr_{min} that this study has used.

The actual Hansen's solubility parameter should be determined for the modified polysulfones to verify the accuracy of the calculated values. If the difference between these values is too great, then parameters more sensitive than Hansen's solubility parameter must be found to compare the difference in adsorptive behavior of polymers.

Testing should be carried out to include non-aqueous solvent systems. This will generalize the concept that there exists a parallel between LC and membrane solution interactions. Important information for solving separation problems in non-aqueous systems could therefore be obtained.

Appendix A

Nomenclature

A	Electrostatic repulsion force constant	(m)
A_m	Molecular cross-sectional area of the adsorbate	(A^2)
a	Activity of a solute	(mol/m^3)
B	Van der Waals attraction force constant	(m^3)
C	Constant for the BET equation	
$b(r)$	frictional parameter	
b	Intercept of a linear equation	
c	Molar concentration	(mol/m^3)
$c_{a,b}$	Molar concentration of solute in the bulk solution	(mol/m^3)
$c_{a,i}$	Molar concentration of solute at the interface	(mol/m^3)
$c_{a,m}$	Molar concentration of solute in the mobile phase	(mol/m^3)
$c_{a,s}$	Molar concentration of solute in the stationary phase	(mol/m^3)
D	Steric repulsion constant	(m)
D_s	Radius of a solute molecule	(m)
D_w	Radius of a water molecule	(m)
d	Distance between polymer material surface and solute molecule center	(m)
f'	Fraction solute separation based on the solute concentration in the boundary phase	
f	Separation based on the feed concentration	
J_a	Molar solute flux	(mol/m^2·s)

K'_a	Equilibrium distribution of a solute between a mobile phase and a stationary phase generated by LC	
$K_{a,i}$	Equilibrium distribution of a solute between a bulk phase and an interfacial layer in a membrane system	
k'_a	Partition coefficent of a solute between a mobile phase and a stationary phase generated by LC	
L	Length of the chromatography column	(cm)
m	Slope	
m_p	Mass of polymer	(g)
N	Avogadro's constant	
N_a	Number of moles of water adsorbed	(mol)
n	Moles of water injected	(mol)
n_0	Moles adsorbed	(mol)
n_{sm}	Mass of Adsorbant per gram of polymer	
$q_{a,m}$	Molar flow rates of a in the mobile phase	(mol/m^3)
$q_{a,s}$	Molar flow rates of a in the mobile phase	(mol/m^3)
P	Pressure	(Kpa)
$P_{o/w}$	Octanol-Water partition coefficient	
R	Universal gas constant	(J/(mole K))
r_c	Critical pore radius	(m)
S_a	Area under a chromatography peak	(cm^3)
S_{locus}	Area obtain from the locus of peak maximia	(cm^3)
T	Temperature	(K)

T_i	Interfacial water thickness	(m)
t_0	Hold-up time for a column	(min)
t_a	Retention time of solute a	(min)
u	Velocity of the mobile phase	(cm/min)
u_a	Velocity of solute a	(m/s)
u_b	Velocity of solvent in pore	(m/s)
V	Carrier flow rate	(cm^3/min)
V_d	Dead volume in a column	(cm^3)
V_{gas}	Volume of gas that pass through a gas chromatography column	(cm^3)
V_m	Volume of the mobile Phase	(cm^3)
V_r	Retention volume	(cm^3)
V_{r_a}	Retention volume of a solute	(cm^3)
V_s	Volume of the Stationary Phase	(cm^3)
v_a	Average mirgration velocity of a	(cm^3/min)
x	Mole fraction of solute in the bulk solution	

Greek Letters

Γ	Surface excess	(mol/m^2)
γ	Interfacial tension	(N/m)
δ	Length of cylindrical pore	(m)
δ_i, δ_j	Adjacent cardinal numbers that describe the carbon-carbon bond in a molecule	
δ_d	Dispersion component solubility parameter	$(J^{\frac{1}{2}}cm^{\frac{3}{2}})$
δ_h	Hydrogen component solubility parameter	$(J^{\frac{1}{2}}cm^{\frac{3}{2}})$
δ_p	Polar component solubility parameter	$(J^{\frac{1}{2}}cm^{\frac{3}{2}})$
δ_t	Total solubility parameter	$(J^{\frac{1}{2}}cm^{\frac{3}{2}})$
$(\delta_t)_e$	Experimentally obtained total solubility parameter	$(J^{\frac{1}{2}}cm^{\frac{3}{2}})$
$(\delta_t)_f$	Total solubility parameter calculated from Fedor's data	$(J^{\frac{1}{2}}cm^{\frac{3}{2}})$
$(\delta_t)_{hv}$	Total solubility parameter calculated from component solubility parameters	$(J^{\frac{1}{2}}cm^{\frac{3}{2}})$
χ_{AB}	Proportionality constant	$(J \cdot s/m^2 \cdot mol)$
χ_{AM}	Membrane solute interaction constant	$(J \cdot s/m^2 \cdot mol)$
$^1\chi$	First order connectivity index	
$\phi(d)$	Potential function	

Subscripts

a	Solute a
$b, 1$	Bulk phase
$i, 2$	Interfacial phase
3	Permeate phase
m	Mobile phase
s	Stationary phase

Bibliography

[1] Osmonic Inc. The filtration spectrum. 1985 Catalogue.

[2] A.W. Adamson. *Physical Chemistry of Surfaces.* John Wiley and Sons, 2nd edition, 1960.

[3] S. Sourirajan. *Reverse Osmosis.* Academic Press, 1970.

[4] M. Kai, K. Ishii, H.T. Tsugaya, and T. Miyano. Development of Polyether Sulfone Ultrafiltration Membranes, *Reverse Osmosis and Ultrafiltration*, edited by S. Sourirajan and T. Matsuura, ACS Symposium series 281, pages 21–33, 1985.

[5] D.R. Llyord, L.E. Gerlowski, C.D. Sunderland, J.P. Wightman, J.E. McGrath, M. Igbal, and Y. Kang. Poly(ary ether) Membranes for Reverse Osmosis, *Synthetic Membranes Vol. II*, edited by A.F. Turbak, ACS Symposium series 154, pages 327-365, 1982.

[6] R.N. Johnson. Polysulfone Resins, *Encyclopedia of Polymer Science and Technology.* Interscience Publishers, Volume 2, 1st edition, pages 447 - 463, 1978.

[7] M.D. Guiver, O. Kutowy, W.A. McCurdy, and J.W. ApSimon. Novel Polysulfones for Membrane Applications, *Proceedings of the International Membrane Conference on the 25th Anniversary of Membrane Research in Canada*, edited by M. Malaiyandi, O. Kutowy, and F. Talbot, pages 187–202. National Research Council, 1986.

[8] M.D. Guiver. *Aromatic Polysulfones Containing Functional Groups by Synthesis and Chemical Modification*, National Research Council of Canada, NRCC No. C1140-875, June 5, 1987.

[9] M.D. Guiver, O. Kutowy, and J. ApSimon. Aromatic polysulfone derivatives and their preparation. U.S. Patent, Application number 932,211, 1986.

[10] M.D. Guiver. *Aromatic Polysulfones Containing Functional Groups by Synthesis and Chemical Modification.* PhD thesis, Carleton University, 1988.

[11] A. Akelah. Review of technological applications of functionalized polymers. *Journal of Material Science*, 21:2977–3001, 1986.

[12] M. Soltanieh and W.N. Gill. Review of reverse osmosis membranes and transport models. *Chemical Engineering Communications*, 12:279–363, 1981.

[13] S. Sourirajan and T. Matsuura. *Reverse Osmosis and Ultralfiltration Process Principles.* National Research Council of Canada, NRCC No. 24188, 1985.

[14] H.K. Lonsdale, U. Merten, and R.L. Riley. Transport porperties of cellulose acetate osmotic membranes. *Journal of Applied Polymer Science*, 9:1341-1362, 1965.

[15] D.H. Everett. Adsorption at the solid/liquid interfaces non-aqueous systems. *Colloid Science*, 1:27–50, 1971.

[16] J.J. Kipling. *Adsorption from Solutions of Non-Electrolytes.* Academic Press, 1965.

[17] T. Matsuura, P. Blais, and S. Sourirajan. Polar and nonpolar parameters for polymeric reverse osmosis membrane materials from liquid chromatography data. *Journal of Applied Polymer Science*, 20:1515–1531, 1976.

[18] T. Matsuura, Y. Taketani, and S. Sourirajan. Estimation of Interfacial Forces Governing the Reverse-Osmosis System Nonionized Polar Organic Solute-Water-Cellulose Acetate Membranes, *Synthetic Membranes Vol. II*, edited by A.F. Turbak, ACS Symposium Series 154, pages 230 - 246.

[19] P.J. Schoenmakers. Optimization of Chromatographic Selectivity: A Guide to Method Developement. *Journal of Chromatography Library*, Volume 35, Elsevier, 1986.

[20] N.A. Paris. Instrumental Liquid Chromatography - A Practical Manual on HPLC Methods. *Journal of Chromatography Library*, Volume 27, 2nd edition, Elsevier, 1981.

[21] R.E. Majors and D.R. Gere. Column theory, *Chromatography*. chapter 3, pages 31–41. Varian Aerography, 1961.

[22] V.K. La Mer, W.C. Eichelberger, and H.C. Urey. *Journal of American Chemical Society*, 56:248–252, 1934.

[23] J.C. Possey and H.A. Smith. *Journal of American Chemical Society*, 79:555–560, 1957.

[24] T. Matsuura, Y. Taketani, and S. Sourirajan. Interfacial parameters governing reverse osmosis for different polymer material-solution systems through gas and liquid chromatography data. *Journal of Colloid and Interface Science*, 95(1):10–22, 1983.

[25] J.F.K. Huber and R.G. Gertise. Evaluation of dynamic gas chromatography methods for the determination of adsorption and solution isotherm. *Journal of Chromatography*, 95(1):137–158, 1971.

[26] U-B. Mohlin and D.G. Gray. Gas chromatography on polymer surfaces adsorption on cellulose. *Journal of Colloid and Interface Science*, 47(3):747–754, 1974.

[27] A.V. Kiselev and Y.I.Yashin. *Gas Adsorption Chromatography*. Plenum Press, 1969.

[28] S.J. Sing and K.S.W. Sing. *Adsorption, Surface Area and Porosity*. Academic Press, 1967.

[29] Y. Taketani, T. Matsuura, and S. Sourirajan. Use of liquid chromatography for studying reverse osmosis and ultrafiltration. *Separation Science and Technology*, 17(6):821–838, 1982.

[30] J. Hazlett, O. Kutowy, T.A. Tweddle, M.D. Guiver and T.W. McCracken. Polysulfone membranes in non-aqueous applications, *Proceedings of the International Membrane Conference on the 25th Anniversary of Membrane Research in Canada*, edited by M. Malaiyandi, O. Kutowy, and F. Talbot, pages 241–257. National Research Council, 1986.

[31] T. Matsuura and S. Sourirajan. *Transport through Reverse Osmosis Membranes.* National Research Council, 1985.

[32] R. Kalizan. *Quantitative Structure-Chromatographic Retention Relationships.* John Wiley and Sons, 1987.

[33] R.F. Rekker. *The Hydro Fragmental Constants - Its Derivation and Applications.* Elsevier, 1977.

[34] C.M. Gary-Bobo, R. DiPolo, and A.K. Solomon. Role of hydrogen-bonding in non-electrolytes diffusion through dense artificial membranes. *Journal of General Physiology*, 54:369, 1969.

[35] Y. Kiso. Factors affecting adsorption of organic solutes on cellulose acetate in an aqueous solution system. *Chromatographia*, 22(1):55, 1986.

[36] Y. Kiso and T. Kitao. Reverse osmosis and liquid chromatography. *Membrane*, 12(5):272–280, 1987.

[37] C. Hansch and A. Leo. *Substituent Constant for Correlation Analysis in Chemistry and Biology.* John Wiley and Sons, 1979.

[38] M. Randic. The structural origin of chromatographic retention data. *Journal of Chromatography*, 161:1–14, 1978.

[39] N. Funasaki, S. Hada, and S. Neya. Prediction of retention times in reverse-phase high performance chromatography from their chemical structures. *Journal of Chromatography*, 361:33-45, 1986.

[40] L.H. Hall and L.B. Kier. Molecular connectivity and substructural analysis. *Journal of Pharmaceutical Science*, 67:1743 - 1747, 1978.

[41] D.W. Van Krevelen. *Properties of Polymers : Their Estimation and Correlation with Chemical Structure*. Elsevier, 2nd edition, 1976.

[42] B.L. Karger, L.R. Snyder, and C. Eon. Expanded solubility parameter treatment for classification and use of chromatographic solvents and adsorbents. *Analytical Chemistry*, 50(14):2126-2136, 1978.

[43] S. Krause. *Partial Solubility Parameter Characterization of Interpenetrating Microphase Membranes*, ACS symposium series 280, pages 351-364, 1985.

[44] C.M. Hansen. The universality of the solubility parameter. *Industrial Engineering Chemistry Process Research and Development*, 8:2, 1969.

[45] T. Miyano. Private communications. NRC unpublished data, 1988.

[46] C.M.Tam, M.D. Guiver, and A.Y. Tremblay. Carboxylate polysulfone membranes membranes. NRC unpublished data, 1988.

[47] R.F. Fedors. A method for estimating both the solubility parameters and the molar volumes of liquids. *Polymer Engineering Science*, 14:147, 1974.

[48] C.M. Tam, M.D. Guiver,and A.Y. Tremblay. Reverse osmosis membranes from novel hydrophilic polysulfones. In : *Symposium of Advances in Reverse Osmosis and Ultrafiltration*, presented at The Third Chemical Congress of North America, Toronto, June 5-10,1988.

[49] A.S. Michaels and S.L. Matson. Membranes in biotechnology : state of the art. *Desalination*, 53:231 - 258, 1985.

[50] E. Drioli. *Membrane Processes in the Separation, Purification, and Concentration of Bioactive Compounds from Fermentation Broths*, ACS symposium series 314, 1986.